A Recursive Algorithm in (t, t') for Quantum Dynamics in the Kramers-Henneberger Frame

Rishabh Gupta

A dissertation submitted for the partial fulfillment of BS-MS dual degree in Science

INDIAN INSTITUTE OF SCIENCE EDUCATION AND RESEARCH, MOHALI

April 2019

Certificate of Examination

This is to certify that the dissertation titled **A Recursive Algorithm in $(\mathbf{t}, \mathbf{t}')$ for Quantum Dynamics in the Kramers-Henneberger Frame of Reference** submitted by **Rishabh Gupta (MS14053)** for the partial fulfilment of BS-MS dual degree programme of the Institute, has been examined by the thesis committee duly appointed by the Institute. The committee finds the work done by the candidate satisfactory and recommends that the report be accepted.

Professor K. S. Viswanathan Dr. R. Ramachandran Dr. P. Balanarayan (Supervisor)

Declaration

The work presented in this dissertation has been carried out by me with Dr. P. Balanarayan at the Indian Institute of Science Education and Research Mohali. This work has not been submitted in part or in full for a degree, a diploma, or a fellowship to any other university or institute. Whenever contributions of others are involved, every effort is made to indicate this clearly, with due acknowledgement of collaborative research and discussions. This thesis is a bonafide record of original work done by me and all sources listed within have been detailed in the bibliography,

Rishabh Gupta
(MS14053)
Dated: 26/04/2019

In my capacity as the supervisor of the candidates project work, I certify that the above statements by the candidate are true to the best of my knowledge.

Dr. P. Balanarayan
(Supervisor)

Acknowledgements

I am grateful to my thesis advisor, Dr. P. Balanarayan, for his support, patience, and encouragement throughout my project. I would also like to thank my project committee members, Professor K. S. Viswanathan and Dr. Ramesh Ramachandran for providing insights that improved the content of this thesis. I deeply express my gratitude to all my fellow lab members, Prashant, Naveen, Nitin, Prateek, Alkit, Mishu, Taseng, Mythreyi, Vishal, Sandeep and Shivam for creating an active work environment and constantly motivating me throughout the duration of the project. I'm also grateful to my close friends, Swadheen, Shashank, Misbah, Akanksha, Amandeep, Joy and Ramandeep for all the rejuvenating moments shared with them outside my workplace. Lastly, with all my heart I would like to thank my parents, brother and sister-in-law for their love, care and constant belief in me all along my journey.

"Nobody ever figures out what life is all about, and it doesn't matter. Explore the world. Nearly everything is really interesting if you go into it deeply enough."

Richard P. Feynmann

"I think I can safely say that nobody understands Quantum Mechanics."

Richard P. Feynmann

Dedicated to My Parents, Brother,

Sister-in-law, and my close friends

For love, support and encouragement

Contents

List of Figures

List of Tables

Abbreviations

a.u.	**a**tomic **u**nits
CW	**C**ontinuous **W**ave
TISE	**T**ime **I**ndependent **S**chrödinger **E**quation
TDSE	**T**ime **D**ependent **S**chrödinger **E**quation
KH	**K**ramers-**H**enneberger
ATI	**A**bove **T**hreshold **I**onization
MPI	**M**ulti **P**hoton **I**onization
TDPT	**T**ime **D**ependent **P**erturbation **T**heory

Physical Constants

Electron rest mass	m_e	=	$9.10938291 \times 10^{-31}$kg
Electron charge	e	=	$1.60217657 \times 10^{-19}$C
Planck's constant	h	=	$6.62607004 \times 10^{-34} m^2 kgs^{-1}$
Reduced Planck's constant	$\hbar$	=	$1.05457182 \times 10^{-34} m^2 kgs^{-1}$
Vacuum permittivity	ϵ_0	=	$8.854187.. \times 10^{-12} Fm^{-1}$ (approximate)

Symbols

a	distance	m
ω	angular frequency	rads^{-1}
ϵ_z	electic field strength	Vm^{-1}
α_0	classical quiver distance	Bohr

Abstract

A quantum system interacting with a high intensity oscillating field can be described by a time periodic semi-classical Hamiltonian. The Floquet theorem and the (t,t′) formalism is employed with the objective to replace the time-dependent Hamiltonian with a time-independent Hamiltonian represented by an infinite matrix. This enables a solution of the time-dependent Schrödinger equation (TDSE) for a quantum system and the time propagation has the advantage of bypassing the complexity of time-ordering operator as chronological ordering is not required for solving TDSE for time-independent Hamiltonians. However, the Floquet prescription of solving the TDSE involves a very heavy diagonalization of Floquet matrix at each time step. To address this problem, a memory and time saving computational scheme in the length gauge has already been suggested earlier which involves the analytical diagonalization of uniform block tri-diagonal matrices. The current work involves the proposition of a novel recursive algorithm in the acceleration gauge, also called the Kramers-Henneberger (KH) frame in the high intensity field regime, to study the quantum dynamics of the system in a linearly polarized laser. The algorithm is tested for two test cases viz. the symmetric double well potential and the xenon model potential. The test calculation validates the proposed recursive algorithm to perform quantum dynamics in the KH frame.

Chapter 1

Introduction

1.1 Light-Matter Interaction

The interaction of an atomic system with laser fields in the intense field regime yields a semi-classical model [1] where the laser-atom interaction is treated classically, and the atom is considered to be a quantum system. The electromagnetic radiation here comprises of time-periodic electric field, $\vec{\epsilon}(\vec{r},t)$, and magnetic field, $\vec{B}(\vec{r},t)$, which can be described from classical scalar and vector potentials given by Maxwell's equations:

$$\vec{\epsilon}(\vec{r},t) = -\nabla\phi(\vec{r},t) - \frac{\partial}{\partial t}\vec{A}(\vec{r},t) \qquad \vec{B}(\vec{r},t) = \nabla \times \vec{A}(\vec{r},t) \tag{1.1}$$

Here $\vec{A}(\vec{r},t)$ and $\phi(\vec{r},t)$ are the vector and scalar potentials, respectively. The dynamics of an atomic system, comprising of a single electron bound by an attractive Coulomb potential,[2] subject to an external classical electromagnetic field, is described by solving the non-relativistic Time-Dependent Schrödinger Equation (TDSE) within the fixed-nucleus (infinite nuclear mass) approximation:[3]

$$i\hbar\frac{\partial\psi(\vec{r},t)}{\partial t} = \hat{H}(\vec{r},t)\psi(\vec{r},t). \tag{1.2}$$

The Hamiltonian, $\hat{H}(\vec{r},t)$, consists of the field-free time-independent term, $\hat{H}^{ff}(\vec{r},t)$, with the kinetic energy and potential energy for the electron, and the time-dependent laser interaction component, $\hat{H}^{1}(\vec{r},t)$ of the form $\vec{\epsilon}(t).\vec{r}$, where $\vec{\epsilon}$ is the electric field component of the electromagnetic field, which is continuous wave (CW) and linearly polarized in nature.
In this description it is important to fix and understand the *gauge dependence* of the solution.

1.1.1 Gauge Transformation

A *gauge transformation* is defined as a unitary transformation that leads to a formal, systematic transformation of the scalar and vector potentials without affecting the physical fields, i.e., the fields should remain invariant under a gauge transformation. According to the Maxwell's equations, there is a vector potential $\vec{A}(\vec{r},t)$ such that on addition of a gradient of arbitrary scalar field, $\chi(\vec{r},t)$, the magnetic field is unchanged.

$$\nabla \ . \ \vec{B} = 0 \qquad \nabla \times \vec{A} = \vec{B} \qquad \vec{A} \rightarrow \vec{A} + \nabla\chi \tag{1.3}$$

From Eq. [1.3], it is inferred that the magnetic field remains invariant upon addition of the gradient of a scalar field $\chi(\vec{r},t)$. Similarly from Eq. [1.4], adding a time derivative of an arbitrary scalar field, $\chi(\vec{r},t)$, to the scalar potential, $\phi(\vec{r},t)$, the electric field remains invariant, as can be seen from Eq. [1.4] (given below) and Eq. [1.3].

$$\nabla \times \vec{E} = -\frac{\partial \vec{B}}{\partial t} \qquad -\nabla\phi - \frac{\partial \vec{A}}{\partial t} = \vec{E} \qquad \phi \rightarrow \phi - \frac{\partial \chi}{\partial t} \tag{1.4}$$

The TDSE should remain invariant upon a gauge transformation so that the measurable atomic properties should not be affected by the transformation. Hence, for the Schrödinger equation to remain unchanged upon the gauge transformation,

the wave function should transform according to the condition:

$$\psi' = e^{-i\chi}\psi. \tag{1.5}$$

In the forthcoming sections, a particular case, very similar to a gauge transformation, called the Kramers-Henneberger (KH) transformation is discussed and a propagation algorithm for this KH is presented. The form of the Hamiltonian used and given in Eq. [1.2] is in the length gauge, after the use of a dipole approximation.

1.1.2 The Dipole Approximation

Generally, the wavelength, λ, of the electromagnetic radiation is considerably larger than the size of an atom.[4] The typical wavelength of the electromagnetic radiation is in the range of few hundred nanometer (nm) and the diameter of an atom ranges from 0.1 nm to 0.5 nm. Therefore, the spatial dependence of the vector potential can be ignored. For a linearly polarized light, the general form of the vector potential is:

$$\vec{A}(\vec{r},t) = f(t)\cos(\vec{k}.\vec{r} - \omega t + \delta_\omega)\vec{\epsilon} \tag{1.6}$$

where $\vec{\epsilon}$ is a unit vector along the direction of polarization of electromagnetic radiation, $\vec{k}$ is the propagation vector with magnitude, $|\vec{k}| = \frac{2\pi}{\lambda}$, ω is the frequency of the oscillating electric field, δ_ω is the initial phase of the system, and $f(t)$ is a time-dependent wave-envelope term. Alternately,

$$\vec{A}(\vec{r},t) = Re\{f(t)e^{i\vec{k}.\vec{r}}e^{i(\omega t-\delta_w)}\vec{\epsilon}\}. \tag{1.7}$$

A Taylor series expansion of $e^{i\vec{k}.\vec{r}}$ yields:

$$e^{i\vec{k}.\vec{r}} = 1 + (i\vec{k}.\vec{r}) + \frac{1}{2}(i\vec{k}.\vec{r})^2 + \dots \tag{1.8}$$

The form of the vector potential on taking only the first two terms of the expansion:

$$\begin{aligned}\vec{A}(\vec{r},t) &\approx \frac{1}{2}f(t)[(1+i\vec{k}.\vec{r})e^{i(\omega t-\delta_w)}+(1-i\vec{k}.\vec{r})e^{-i(\omega t-\delta_w)}]\vec{\epsilon} \\ &\approx f(t)[\cos\omega t+\vec{k}.\vec{r}\sin(\omega t)]\vec{\epsilon} \;\;;\;\; \delta_w=0 \\ &\approx \vec{A^0}(t)+\vec{A^1}(\vec{r},t). \end{aligned} \tag{1.9}$$

Here, $\vec{A^0}(t)$ is the spatially independent vector potential within the dipole approximation and $\vec{A^1}(\vec{r},t)$ is the correction term. Since the size of an atom is very small as compared to the wavelength of the electromagnetic radiation so the correction term can be ignored. As a result, the vector potential is set to be:

$$\vec{A}(\vec{r},t)=f(t).\cos\omega t\vec{\epsilon}. \tag{1.10}$$

Since, the vector potential has only a temporal dependence within the dipole approximation, the magnetic field $\vec{B}(\vec{r},t)$ vanishes from Eq. [1.1] and the electric field $\vec{\epsilon}(t)$ is given by:

$$\vec{\epsilon}(t)=-\frac{d\vec{A}(t)}{dt} \tag{1.11}$$

For a CW laser, the time-dependent wave envelope function, $f(t)$=1. Hence, in the Coulomb gauge, the TDSE for a single electron in an attractive Coulomb potential $V(\vec{r})$ subject to an external oscillating electric field is:

$$i\hbar\frac{\partial\psi(\vec{r},t)}{\partial t}=\left[-\frac{\hbar^2}{2m_e}\hat{\nabla}^2+\vec{\epsilon}(t).\vec{r}+V(\vec{r})\right]\psi(\vec{r},t) \tag{1.12}$$

Having defined the Hamiltonian, the forthcoming sections will describe various experiments and phenomenon related to light-matter interaction in the strong field regimes.

1.2 Electronic Response to Lasers

Atoms subject to ordinary light beams tend to ionize with a small probability. From the quantum description of an atom, there is a discretization of the atomic energy levels. When a photon of energy $\hbar\omega$, interacts with the atom, the result is ionization, provided $\hbar\omega$ is greater than the ionization potential of the atom. If the intensity of the light beam is increased, the probability of ionization also rises owing to the increased interactions between the photons and atoms resulting in stripping off the outermost electron leading to ionization. A brief overview of the basic phenomenology of ionization in the weak to strong intensity regimes of the laser is presented in the following section.

1.2.1 Light induced Ionization Processes

1. **Single photon ionization:** The interaction of an atom with a photon whose frequency matches with or exceeds the ionization energy (threshold frequency) of the atom leads to its photoionization.[5, 6] The excess energy above the threshold is imparted to the ejected electron in the form of kinetic energy. This phenomenon is called *single photon ionization.*

2. **Multiphoton ionization:** In the weak field regime, ionization process predominantly takes place through single photon ionization phenomenon. However, as the intensity of laser field is increased, typically above 10^{13} W/cm^2, the frequency of laser need not be over the atom's ionization potential and the bound electron can absorb multiple photons leading to ionization of the electron.[7–11] This process is termed as *multiphoton ionization.*

3. **Above-threshold ionization:** The *above-threshold ionization* (ATI) is an unexpected phenomenon in multi-photon physics wherein the bound electron absorbs a larger number of photons than what is expected for its ionization.[12] The simultaneous phase-coherence between the electron and the parent ion along with the laser light for laser intensities above 1 TW/cm^2 gives rise to ATI. This implies that the ionizing electron absorbs photons

while still interacting with the parent ion which provides the necessary momentum transfer.[13]

4. **Tunneling ionization:** In the high intensity, low-frequency regime, the bound valence electron experiences a quasi-static potential [14] created by the superposition of the attractive Coulomb potential of the ionic core and the instantaneous electric field potential $V_E = \vec{\epsilon}(t).\vec{r}$. The strong laser field intensity perturbs the binding potential to such an extent that allows the electron to tunnel through a transformed barrier leading to ionization. This phenomenon is known as *tunnel ionization.*

Both multiphoton ionization and tunneling ionization occur in the high-intensity regime of the laser field. The multiphoton ionization process occurs at a high frequency of laser field as the probability of ionization is higher with a fewer number of high energy photons, since according to perturbation theory the absorption of fewer photons is more likely as the probability of many photons interacting with the atom at the same instant is very shallow.[15] However, for the bound electron to tunnel through the barrier potential the tunneling time scale should be shorter than the inverse frequency of the radiation. Therefore, for tunneling, the laser frequency should be low.[16] Thus, the two ionization processes occur at different regimes of the laser frequency spectrum.
Keldysh [14] gave a quantitative measure of the possibility of occurrence of the two strong-field ionization mechanisms and proposed a general analytical expression, known as the Keldysh parameter or the adiabaticity parameter,

$$\gamma = \omega \frac{\sqrt{2m_e V_{IE}}}{eE}. \tag{1.13}$$

Here ω is the angular frequency of the laser, V_{IE} is the zero-field ionization energy of the system, m_e and e are the mass and charge of the electron. For the electron to tunnel through the potential barrier, the tunneling condition is such that the Keldysh parameter, $\gamma \ll 1$ whereas for multiphoton ionization $\gamma > 1$.[17] Thus, the Keldysh parameter, γ, is a measure of whether the electron may be able to tunnel through the time-periodically created potential barrier or not.

1.3 Atomic Stabilization by Super-Intense Lasers

Over the past few decades, it has been shown that when an atom is subject to high values of laser frequency and laser intensity typically of the order of 10^{16} W/cm^2, there is an unexpected behavior in contrast to the ionization that is expected.[18] In fact, the stripping rate of electron slows down dramatically [19] as the laser intensity is increased above a critical point, and the atomic wave function assumes a bi-lobal form. This bi-lobal form continues to exist as the laser intensity increases, and hence, this new atomic configuration is referred to as *stabilized*. The process has become known as *atomic stabilization*.

The interaction of super-intense laser fields with an atom can be analyzed in a sense that the atom is supersaturated with photons which leads to modification of both its bound and free states. Thus, the photo-initiated processes such as ATI and high harmonic generation cease to be defined in terms of one or two or any well-defined individual photons but rather are defined in terms of an effective electric field of collective photons. Consequently, the atom in strong laser fields is commonly referred to as *laser-dressed* atom. In this regime, highly coherent and very high order momentum-transfer collisions contribute to the exchange of energy between the field and the electron instead of photon absorption and thus, shifts the energies of bound and free states of the atom by causing the electron to oscillate with the field. Considering this reasoning, the super-intense laser is better characterized as a light wave instead of a beam of bullet-like photons.

The dynamic electric force of the high-intensity laser renders the protons' attractive force to be ineffective and compels the electron to move back and forth along the straight line in the direction of laser polarization and thus very effectively traps it in this new orbit. A key insight in understanding the detailed quantum dynamics of stabilization was provided by Henneberger,[2] Mittleman,[19] and Gavrila,[18] and the idea was based on even earlier work by Kramers [20] and by Pauli and Fierz [21] in the 1930s on the fundamental theory of quantum electrodynamics.

1.4 The Kramers-Henneberger Atom

Atomic systems in the presence of strong laser fields undergo distortion, along with the ionization process as a result of the absorption of photons.[22] With an increase in the laser field intensity, the distortion is accompanied with a decrease in the ionization probability which amounts to increase in the stabilization of the atomic system. The Coulomb binding potential of the atom is suppressed by the laser field and with sufficiently high intensity, the electron, which was earlier confined within the potential well, becomes nearly free to oscillate with the frequency of the laser. The dynamics of such a system is more appropriately described if the coordinate system is fixed on the moving electron. This moving coordinate frame is generally called the Kramers-Henneberger (KH) frame of reference.
The spatial transformation to the KH frame is the first step to deal with laser-atom interaction in the high-intensity and high-frequency regime. The instantaneous velocity of the oscillating potential at the turning points is zero, and therefore, those points are the most probable positions for the laser-driven electron. The time-average of the oscillating potential yields a symmetric double-well potential called the KH potential and the laser-dressed atom is called the KH atom. This transformed KH potential is capable of supporting infinitely many bound states of the KH atom.[23] The new basis obtained by this transformation into the KH frame adequately describes most of the laser-atom interaction and the rest can be implemented as perturbations.

1.5 The Kramers-Henneberger Transformation

1.5.1 Transformation to the momentum gauge

This section comprises of the formal description of the transformation of the TDSE from the length gauge to the acceleration gauge. The TDSE in the length gauge

for an electron in the presence of an oscillating electric field is given as ($\hbar$=1):

$$i\frac{\partial}{\partial t}\psi(\vec{r},t) = \Big[-\hat{\nabla}^2/2 + V(\vec{r}) + \epsilon_0 \hat{e}_z.\vec{r}\cos\omega t\Big]\psi(\vec{r},t) \tag{1.14}$$

Let $\psi(\vec{r},t) = \hat{U}\hat{U}^\dagger\psi(\vec{r},t)$, where $\hat{U}$ is the unitary operator which transforms the wave function from the length gauge to the momentum gauge.
Now, $\psi(\vec{r},t) = \hat{U}\psi'(\vec{r},t)$, where $\psi'(\vec{r},t) = \hat{U}^\dagger\psi(\vec{r},t)$. Substituting it in the TDSE in Eq.[1.14], we obtain:

$$\begin{aligned} i\frac{\partial\hat{U}\psi'(\vec{r},t)}{\partial t} &= \Big[-\hat{\nabla}^2/2 + V(\vec{r}) + \epsilon_0 \hat{e}_z.\vec{r}\cos\omega t\Big]\hat{U}\psi'(\vec{r},t) \\ i\hat{U}\frac{\partial\psi'(\vec{r},t)}{\partial t} + i\frac{\partial\hat{U}}{\partial t}\psi'(\vec{r},t) &= \Big[-\hat{\nabla}^2/2 + V(\vec{r}) + \epsilon_0 \hat{e}_z.\vec{r}\cos\omega t\Big]\hat{U}\psi'(\vec{r},t) \end{aligned} \tag{1.15}$$

Therefore, on choosing the following form of the unitary operator:

$$\hat{U} = \exp[-i\frac{\epsilon_0\hat{e}_z.\vec{r}}{\omega}\sin\omega t] \tag{1.16}$$

the interaction can be modified. Since,

$$\begin{aligned} i\hat{U}\frac{\partial\psi'(\vec{r},t)}{\partial t} &= \Big[-\hat{\nabla}^2/2 + V(\vec{r})\Big]\hat{U}\psi'(\vec{r},t) \\ i\frac{\partial\psi'(\vec{r},t)}{\partial t} &= \hat{U}^\dagger\Big[-\hat{\nabla}^2/2 + V(\vec{r})\Big]\hat{U}\psi'(\vec{r},t) \end{aligned} \tag{1.17}$$

From Baker-Campbell-Hausdroff formula, we have:

$$\exp[\hat{A}]\hat{B}\exp[-\hat{A}] = \hat{B} + [\hat{A},\hat{B}] + [\hat{A},[\hat{A},\hat{B}]]/2! + \ldots \tag{1.18}$$

Calculating $\hat{U}^\dagger\Big[-\hat{\nabla}^2/2 + V(r)\Big]\hat{U}$:

$$\begin{aligned} \Rightarrow \exp[-i\frac{\epsilon_0\hat{e}_z.\vec{r}}{\omega}\sin\omega t](-\hat{\nabla}^2/2)\exp[i\frac{\epsilon_0\hat{e}_z.\vec{r}}{\omega}\sin\omega t] \\ + \exp[-i\frac{\epsilon_0\hat{e}_z.\vec{r}}{\omega}\sin\omega t](V(\vec{r}))\exp[i\frac{\epsilon_0\hat{e}_z.\vec{r}}{\omega}\sin\omega t] \end{aligned}$$

$$\begin{aligned}
\Rightarrow \quad & -\hat{\nabla}^2/2 + i\frac{\epsilon_0}{\omega}\sin\omega t[\vec{r}, -\hat{\nabla}^2/2] + \frac{\epsilon_0^2}{\omega^2}\sin^2\omega t[\vec{r},[\vec{r}, -\hat{\nabla}^2/2]]/2! + \ldots \\
& + \; V(\vec{r}) + i\frac{\epsilon_0}{\omega}\sin\omega t[\vec{r}, V(\vec{r})] + \frac{\epsilon_0^2}{\omega^2}\sin^2\omega t[\vec{r},[\vec{r}, V(\vec{r})]]/2! + \ldots \\
\Rightarrow \quad & -\hat{\nabla}^2/2 + i\frac{\epsilon_0}{\omega}\sin\omega t(\hat{\nabla}) + \frac{\epsilon_0^2}{\omega^2}\sin^2\omega t(k) + V(\vec{r})
\end{aligned}$$

where $k = [\vec{r},[\vec{r}, -\hat{\nabla}^2/2]]/2! = constant$ and hence, the third term contribute only to a phase factor and so, it can be ignored. Therefore,

$$\hat{U}^\dagger\Big[-\hat{\nabla}^2/2 + V(\vec{r})\Big]\hat{U} = -\hat{\nabla}^2/2 + i\frac{\epsilon_0}{\omega}\sin\omega t\hat{\nabla} + V(\vec{r}) \tag{1.19}$$

Putting it in Eq. [1.17], we obtain:

$$i\frac{\partial\psi'(\vec{r},t)}{\partial t} = \Big[-\hat{\nabla}^2/2 + i\frac{\epsilon_0}{\omega}\sin\omega t\hat{\nabla} + V(\vec{r})\Big]\psi'(\vec{r},t) \tag{1.20}$$

Thus the TDSE is transformed from the length gauge to the momentum gauge and the next step is to further transform Eq. [1.20] to the *acceleration gauge*.

1.5.2 Transformation to the *acceleration gauge*

Let $\psi'(\vec{r},t) = \hat{U}\hat{U}^\dagger\psi'(\vec{r},t)$, where $\hat{U}$ is the unitary operator which transforms the wave function from the momentum gauge to the *acceleration gauge*.
Now, $\psi'(\vec{r},t) = \hat{U}\psi_{KH}(\vec{r},t)$, where $\psi_{KH}(\vec{r},t) = \hat{U}^\dagger\psi'(\vec{r},t)$. Substituting it in Eq. [1.20] gives:

$$\begin{aligned}
i\frac{\partial\hat{U}\psi_{KH}(\vec{r},t)}{\partial t} &= \Big[-\hat{\nabla}^2/2 + i\frac{\epsilon_0}{\omega}\sin\omega t\hat{\nabla} + V(\vec{r})\Big]\hat{U}\psi_{KH}(\vec{r},t) \\
i\hat{U}\frac{\partial\psi_{KH}(\vec{r},t)}{\partial t} + i\frac{\partial\hat{U}}{\partial t}\psi_{KH}(\vec{r},t) &= \Big[-\hat{\nabla}^2/2 + i\frac{\epsilon_0}{\omega}\sin\omega t\hat{\nabla} + V(\vec{r})\Big]\hat{U}\psi_{KH}(\vec{r},t)
\end{aligned}$$

Therefore, the following form of the unitary operator is obtained:

$$\hat{U} = \exp[\frac{\epsilon_0}{\omega^2}\cos\omega t\nabla] \tag{1.21}$$

Since,

$$\begin{aligned} i\hat{U}\frac{\partial\psi_{KH}(\vec{r},t)}{\partial t} &= \Big[-\hat{\nabla}^2/2 + V(\vec{r})\Big]\hat{U}\psi_{KH}(\vec{r},t) \\ i\frac{\partial\psi_{KH}(\vec{r},t)}{\partial t} &= \hat{U}^\dagger\Big[-\hat{\nabla}^2/2 + V(\vec{r})\Big]\hat{U}\psi_{KH}(\vec{r},t) \end{aligned} \tag{1.22}$$

From Baker-Campbell-Hausdroff formula, calculating $\hat{U}^\dagger\Big[-\hat{\nabla}^2/2 + V(\vec{r})\Big]\hat{U}$:

$$\begin{aligned} \Rightarrow\quad & \exp^{i\frac{\epsilon_0}{\omega^2}\cos\omega t\hat{\nabla}}(-\hat{\nabla}^2/2)\exp^{-i\frac{\epsilon_0}{\omega^2}\cos\omega t\hat{\nabla}} + \exp^{i\frac{\epsilon_0}{\omega^2}\cos\omega t\hat{\nabla}}(V(\vec{r}))e^{-i\frac{\epsilon_0}{\omega^2}\cos\omega t\hat{\nabla}} \\ \Rightarrow\quad & -\hat{\nabla}^2/2 + i\frac{\epsilon_0}{\omega^2}\cos\omega t[\hat{\nabla},-\hat{\nabla}^2/2] + \frac{\epsilon_0^2}{\omega^4}\cos^2\omega t[\hat{\nabla},[\hat{\nabla},-\hat{\nabla}^2/2]]/2! + \ldots \\ & + \quad V(\vec{r}) + i\frac{\epsilon_0}{\omega^2}\cos\omega t[\hat{\nabla},V(\vec{r})] + \frac{\epsilon_0^2}{\omega^4})\cos^2\omega t[\hat{\nabla},[\hat{\nabla},V(\vec{r})]]/2! + \ldots \\ \Rightarrow\quad & -\hat{\nabla}^2/2 + V(\vec{r}) + \frac{\epsilon_0}{\omega^2}\cos\omega t\hat{\nabla}V(\vec{r}) + \frac{\epsilon_0^2}{2!\omega^4}\cos^2\omega t\hat{\nabla}^2V(\vec{r}) + \ldots \\ \Rightarrow\quad & -\hat{\nabla}^2/2 + V(\vec{r}+\alpha\cos\omega t) \quad ; \qquad \alpha = \frac{\epsilon_0}{\omega^2} \end{aligned}$$

Therefore,

$$\hat{U}^\dagger\Big[-\hat{\nabla}^2/2 + V(\vec{r})\Big]U = -\hat{\nabla}^2/2 + V(\vec{r}+\alpha\cos\omega t) \tag{1.23}$$

Substituting it in Eq. [1.22] gives:

$$i\frac{\partial\psi_{KH}(\vec{r},t)}{\partial t} = \Big[-\hat{\nabla}^2/2 + V(\vec{r}+\alpha\cos\omega t)\Big]\psi_{KH}(\vec{r},t) \tag{1.24}$$

Thus, the TDSE is transformed from the momentum gauge to the acceleration gauge. This thesis deals with an algorithm for time evolution in the KH frame given in Eq. [1.24]. The next set of sections review basic methodologies involved in solving TDSE.

1.6 Methods of solving TDSE with time-dependent Hamiltonian

A comparative study of different propagation schemes for the TDSE in case of time-independent Hamiltonians by Kosloff and co-workers [25] in 1990 demonstrates the accuracy and efficiency of different methods on a numerical grid. The different methods considered for studying the evolution of the system were: second-order differencing,[26] split-operator propagation,[27] Chebyshev polynomial expansion method.[28] A new method, based on low-order Lanczos technique [25] was also introduced in the case of time-dependent potentials which proved to be an accurate and flexible alternative to the existing techniques.

In 1993, a novel powerful computational tool, the (t, t') method, was introduced by Peskin and Moiseyev [32] for the solution of TDSE with time-dependent Hamiltonians. Their time propagation methodology included the conversion of time-dependent Hamiltonian into a time-independent Hamiltonian by employing the Floquet theorem and the (t, t') formalism and thereby using the Chebyshev polynomial expansion method for implementation of the method on a numerical grid. The current thesis work incorporates the (t, t') formalism for studying the dynamics of wavepacket in the KH gauge.

A time-dependent potential emerges out of the interaction of laser fields with a quantum system. There have been various methods of solving the TDSE for such a system like the Time-Dependent Perturbation Theory (TDPT), the Magnus expansion method, etc.[24] In this section, a brief description of the TDPT, the time-ordering operator and the Magnus expansion is provided along with a formal elaborate description of the (t, t') method which is employed in this thesis work to solve the TDSE.

1.6.1 Time-Dependent Perturbation Theory

Let us consider a quantum system whose Hamiltonian is described by $\hat{H} = \hat{H}_0 + \hat{H}_1(t)$, where $\hat{H}_0$ is time-independent, and $\hat{H}_1$ need not be. Also, it is assumed that

we can compute the time evolution of a wavepacket under consideration generated by $\hat{H}_0$. Then, under the condition that $\hat{H}_1 \ll \hat{H}_0$, the TDPT can be applied to study the time evolution of the quantum system.[24] An ordering parameter, λ, is introduced to collect the terms that are in similar orders of the perturbation:

$$\hat{H} = \hat{H}_0 + \lambda \hat{H}_1 \tag{1.25}$$

The wavepacket is then expanded in a power series of λ:

$$\psi(t) = \psi^{(0)}(t) + \lambda\psi^{(1)}(t) + \lambda^2\psi^{(2)}(t) + \ldots = \sum_n \lambda^n \psi^{(n)}(t) \tag{1.26}$$

Substituting the expansion in the TDSE and equating the like power terms of λ, a series of equations is obtained:[24]

$$\begin{aligned} i\hbar\frac{\partial}{\partial t}\psi^{(0)} &= \hat{H}_0\psi^{(0)} \\ i\hbar\frac{\partial}{\partial t}\psi^{(1)} &= \hat{H}_0\psi^{(1)} + \hat{H}_1\psi^{(0)} \\ i\hbar\frac{\partial}{\partial t}\psi^{(2)} &= \hat{H}_0\psi^{(2)} + \hat{H}_1\psi^{(1)} \end{aligned}$$

and so on. Solving these equations yields the correction terms:

$$\begin{aligned} \psi^{(0)}(t) &= e^{-\frac{i}{\hbar}\hat{H}_0(t-t_0)}\psi^{(0)} \\ \psi^{(1)}(t) &= \frac{1}{i\hbar}\int_{t_0}^{t} e^{\frac{i}{\hbar}\hat{H}_0 t'}\hat{H}_1(t')\psi^{(0)}(t')dt' + e^{\frac{i}{\hbar}\hat{H}_0(t-t_0)}\psi^{(1)}(t_0) \\ \psi^{(2)}(t) &= \frac{1}{i\hbar}\int_{t_0}^{t} e^{\frac{i}{\hbar}\hat{H}_0 t'}\hat{H}_1(t')\psi^{(1)}(t')dt' + e^{\frac{i}{\hbar}\hat{H}_0(t-t_0)}\psi^{(2)}(t_0) \end{aligned}$$

Generally, for finite time perturbation, $t_0 = 0$ defining the zero of time to be before the perturbation takes effect and so it is assumed that $\psi(t_0) = \psi^{(0)}(t_0)$ and $\psi^{(1)}(t_0) = \psi^{(2)}(t_0) = 0$. On substituting the correction terms in Eq. [1.26] the wave function of the evolved quantum system is evaluated.

1.6.2 Time-ordering Operator and the Magnus Expansion

Solving of the TDSE yields the following solution for the time evolution of an initial state ψ(x,0):

$$\psi(x,t) = e^{-i\hat{H}t/\hbar}\psi(x,0) \tag{1.27}$$

The above propagator operator is only valid when the Hamiltonian is time-independent. In the case of time-dependent Hamiltonian, one might generalize the evaluation of the propagator by integrating the Hamiltonian over time.

$$\psi(x,t) = e^{-i\int_0^t \hat{H}(t')dt'/\hbar}\psi(x,0) \tag{1.28}$$

However, the above assumption is not correct. Taking the Taylor series expansion of the exponential gives:

$$\psi(x,t) = \psi(x,0) - \frac{i}{\hbar}\int_0^t \hat{H}(t')dt'\psi(x,0) - \frac{1}{2\hbar^2}\int_0^t\int_0^t \hat{H}(t')\hat{H}(t'')dt'dt''\psi(x,0) + \dots$$

The above equation maintains that $\hat{H}(\mathrm{t}')$ always acts on $\psi(x,0)$ after $\hat{H}(\mathrm{t}'')$, regardless of whether $t' > t''$ or not, whereas from the differential form of TDSE the Hamiltonian at different times must act on the wave function in chronological order. Thus, an operator is introduced to maintain this chronological ordering:

$$\psi(x,t) = \hat{T}e^{-i\hat{H}t/\hbar}\psi(x,0) \tag{1.29}$$

where $\hat{T}$ is the time-ordering operator.[24] Since the Hamiltonian at different time steps does not commute, there result error terms equivalent to the commutator of the Hamiltonians at those time steps. Typically, one would want to express the propagator in the form of an exponential function as:

$$\hat{U}(t,0) = \exp[\hat{A}(t)], \hat{A}(t) = \hat{A}_1(t) + \hat{A}_2(t) + \hat{A}_3(t) + \dots \tag{1.30}$$

This is carried out by the Magnus expansion. The first few $\hat{A}$'s are of the form:

$$\begin{aligned}
\hat{A}_1 &= \frac{1}{i\hbar}\int_0^t dt_1 \hat{H}(t_1) \\
\hat{A}_2 &= -\frac{1}{2}(\frac{1}{i\hbar})^2 \int_0^t dt_2 \int_0^{t_2} dt_1 [\hat{H}(t_1), \hat{H}(t_2)] \\
\hat{A}_3 &= -\frac{1}{6}(\frac{1}{i\hbar})^3 \int_0^t dt_3 \int_0^{t_3} dt_2 \int_0^{t_2} dt_1 [\hat{H}(t_1), [\hat{H}(t_2), \hat{H}(t_3)]] \\
&+ [[\hat{H}(t_1), \hat{H}(t_2)], \hat{H}(t_3)]
\end{aligned}$$

The leading term, $\hat{A}_1$, is of the form expected in Eq. [1.28]. The higher order correction terms are consistent with the observation that the error term should involve the commutator of $\hat{H}(\mathrm{t}_1)$ and $\hat{H}(\mathrm{t}_2)$, and so forth such that the operation of the Hamiltonian on the wave function is correctly time-ordered.

In order to avoid the complexity of the time-ordering operator, another methodology to solve the TDSE is to convert the time-dependent Hamiltonian into an infinite dimensional time-independent Hamiltonian by employing the Floquet method. Therefore, in the subsequent sections, the basics of the Floquet theorem is discussed along with its implementation on the KH atom. This is followed by a formal description of the (t, t') method which incorporates the Floquet description of a Hamiltonian into its formalism.

1.7 Basic Floquet Theory

Objective: To address the problem of the form:[29]

$$x' = A(t)x \tag{1.31}$$

where $A(t)$ is periodic with period T and is of the form $f(t)\cos\omega t$, where $f(t)$ is a time-dependent wave-envelope function. The interaction of an atomic system in the presence of laser fields yields a time-periodic Hamiltonian whose TDSE is representative of the above differential equation, so it is imperative to address the methodology of solving such an equation.

According to Floquet theorem, the solution x of the above differential equation need not be periodic and is of the form:

$$e^{\mu t}P(t) \tag{1.32}$$

Here P(t) is periodic with period T. The n solutions of the differential equation has n such μ_j and together they satisfy:

$$e^{\mu_1 T}e^{\mu_2 T}\dots e^{\mu_n T} = exp\bigg(\int_0^T tr(A(s))ds\bigg). \tag{1.33}$$

Definition (Fundamental Matrix): Let $\mathrm{x}^1(t),\dots,x^n(t)$ be n solutions of $x' = A(t)x$. Let

$$X(t) = \bigg[\bigg[x^1\bigg]\dots\bigg[x^n\bigg]\bigg] \tag{1.34}$$

so that $X(t)$ is an $n * n$ matrix solution of $X' = AX$.
$X(t)$ is non-singular for linearly dependent $x^1(t),\dots,x^n(t)$ and is called *fundamental matrix*. $X(t)$ is the principal fundamental matrix for $X(t_0) = I$.

Lemma 1: If $X(t)$ is a fundamental matrix then so is $Y(t) = X(t)B$ for any non-singular constant matrix B.
Proof: Since $X(t)$ and B are non-singular then the inverse of $Y(t)$ is $B^{-1}X^{-1}(t)$ and so $Y(t)$ is non-singular. Also,

$$Y' = X'B = AXB = AY \tag{1.35}$$

so that $Y'(t) = AY(t)$.

Lemma 2: Let the *Wronskian* W(t) of X(t) be the determinant of X(t). Then:[29]

$$W(t) = W(t_0)exp\bigg(\int_{t_0}^t tr(A(s))ds\bigg). \tag{1.36}$$

Proof: Let t_0 be some time. Expanding in Taylor series,

$$\begin{aligned} X(t) &= X(t_0) + (t-t_0)X'(t_0) + \mathcal{O}((t-t_0)^2) \\ &= X(t_0) + (t-t_0)A(t_0)X(t_0) + \mathcal{O}((t-t_0)^2) \\ &= [I + (t-t_0)A(t_0)]X(t_0) + \mathcal{O}((t-t_0)^2) \end{aligned} \tag{1.37}$$

so that

$$\begin{aligned} det(X(t)) &= det[I + (t-t_0)A(t_0)]det(X(t_0) \\ W(t) &= det[I + (t-t_0)A(t_0)]W(t_0). \end{aligned} \tag{1.38}$$

Now since

$$det(I + \epsilon C) = 1 + \epsilon tr(C) + \mathcal{O}(\epsilon^2), \tag{1.39}$$

we have that

$$W(t) = W(t_0)(1 + (t-t_0)tr(A(t_0). \tag{1.40}$$

Now by expanding W(t) in a Taylor series, we obtain that

$$W(t) = W(t_0) + (t-t_0)W'(t_0) + \mathcal{O}((t-t_0)^2) \tag{1.41}$$

so that

$$W'(t_0) = W(t_0)tr(A(t_0)). \tag{1.42}$$

Since we have not made any assumptions about t_0), we can then write

$$W'(t) = W(t)tr(A(t)). \tag{1.43}$$

We know the solution to this equation is

$$W(t) = W(t_0)exp\bigg(\int_{t_0}^{t} tr(A(s))ds\bigg) \tag{1.44}$$

Theorem: Let $A(t)$ be a T-periodic matrix. If $X(t)$ is a fundamental matrix then so is $X(t+T)$ and there exist a non-singular constant matrix B such that:
(1) X(t+T) = X(t)B for all t
(2) det(B) = $exp\bigg(\int_0^T tr(A(s))ds\bigg)$
Proof: The first step is to show that $X(t+T)$ is also a fundamental matrix. Let $Y(t) = X(t+T)$. Then

$$Y'(t) = X'(t+T) = A(t+T)X(t+T) = A(t)X(t+T) = A(t)Y(t) \tag{1.45}$$

and so $X(t+T)$ is also a fundamental matrix.
(1) Let $B(t) = X^{-1}(t)Y(t)$. Then

$$\begin{aligned} Y(t) &= X(t)X^{-1}(t)Y(t) \\ &= X(t)B(t) \end{aligned} \tag{1.46}$$

Let $B_0 = B(t_0)$. From lemma 1 $Y_0(t) = X(t)B_0$ is a fundamental matrix, where, by definition, $Y_0(t_0) = Y(t_0)$. Since these are both solutions to $X' = AX$, by the uniqueness of the solution, we must then have $Y_0(t) = Y(t)$ for all time. As a result, $B_0 = B(t)$ and so B is time-independent. (2) From Lemma 2, we have that

$$\begin{aligned} W(t) &= W(t_0)exp\bigg(\int_{t_0}^{t} tr(A(s))ds\bigg) \\ W(t+T) &= W(t_0)exp\bigg(\int_{t_0}^{t} tr(A(s))ds + \int_{t}^{t+T} tr(A(s))ds\bigg) \qquad (1.47) \\ W(t+T) &= W(t)exp\bigg(\int_{t}^{t+T} tr(A(s))ds\bigg) \\ W(t+T) &= W(t)exp\bigg(\int_{0}^{T} tr(A(s))ds\bigg) \qquad (1.48) \end{aligned}$$

We also know that

$$\begin{aligned} X(t+T) &= X(t)B \\ det(X(t+T)) &= det(X(t))det(B) \\ W(t+T) &= W(t)det(B) \end{aligned} \tag{1.49}$$

and so

$$det(B) = exp\bigg(\int_0^T tr(A(s))ds\bigg) \tag{1.50}$$

Since B is time-independent, it can be computed by setting t = 0, so that $B = X^{-1}(0)X(T)$. If we take the initial conditions $X(0) = I$, then $B = X(T)$.

1.8 The Floquet Method for the Kramers-Henneberger Atom

The Floquet method to solve the TDSE for time-periodic Hamiltonian is carried out by extending the Hilbert space such that it comprises of a complete basis in both position and time.

To get an insight into the dynamics of a quantum system, it is important to solve the TDSE in matrix form for the time-periodic Hamiltonian $\hat{H}$ with period T($\omega T = 2\pi$)($\hbar = 1$).

$$i\frac{\partial\psi(\vec{r},t)}{\partial t} = \hat{H}(\vec{r},t)\psi(\vec{r},t) \tag{1.51}$$

The solution of the above equation is expressed in terms of basis functions:

$$\psi(\vec{r},t) = \sum c_k\psi_k(\vec{r},t) \tag{1.52}$$

The form of the basis functions using the Floquet's theorem is given by:[2]

$$\psi_k(\vec{r},t) = e^{-iE_kt}\phi_k(\vec{r},t) \tag{1.53}$$

Here, ϕ is a matrix of periodic functions of t and E is a constant diagonal matrix whose elements are called the characteristic exponents. ϕ_k is expanded in the basis of the Fourier series to obtain the following expression of the solution:

$$\psi_k(\vec{r},t) = \sum_{n=-\infty}^{\infty}\sum_{j=1}^{\infty} e^{-iE_kt}e^{in\omega t}\chi_j(r) \tag{1.54}$$

Substituting this solution in the TDSE gives($\hbar = 1$):

$$\{\hat{H}(\vec{r},t) - i\frac{\partial}{\partial t}\}\phi_k(\vec{r},t) = E_k\phi_k(\vec{r},t) \tag{1.55}$$

$\phi_k(\vec{r}$,t) are called the Floquet eigenstates and $\{\hat{H}(\vec{r},t) - i\frac{\partial}{\partial t}\}$ is the Floquet Hamiltonian represented by $\hat{H}_F(\vec{r}$,t).

Let us now consider a quantum system, whose Hamiltonian operator is $\hat{H}$, which is perturbed using an oscillating electric field such that the Floquet Hamiltonian is given by $hat H_F = \hat{H} - i\frac{\partial}{\partial t} + \epsilon_0 x cos\omega t$. The Floquet Hamiltonian is expanded in matrix notation using the basis given in Eq. [1.54]:

$$\begin{aligned}\langle\langle\psi_\alpha|\hat{H}_F|\psi_\beta\rangle\rangle &= \langle\langle\sum_{n=1}^{\infty}\sum_{j=1}^{\infty} e^{-iE_\alpha t}e^{in\omega t}\phi_j(r)|\hat{H} - i\frac{\partial}{\partial t} + \epsilon_0 x cos\omega t| \\ &\quad \sum_{n'=1}^{\infty}\sum_{j'=1}^{\infty} e^{-iE_\beta t}e^{in'\omega t}\phi_{j'}(r)\rangle\rangle \\ &= \delta_{n,n'}H_{\alpha\beta} + \delta_{j,j'}\delta_{n,n'}n\omega + \delta_{n,n'\pm1}D\end{aligned} \tag{1.56}$$

The elements of the Floquet matrix are defined as :

$$H_{\alpha\beta} = \frac{1}{T}\int_0^T \langle\alpha|\hat{H}(\vec{r},t)|\beta\rangle dt = \langle\alpha|\overline{H}(\vec{r})|\beta\rangle \tag{1.57}$$

where $\overline{H}(\vec{r})$ is the time averaged Hamiltonian.

$$D_{\alpha\beta} = \frac{1}{T}\int_0^T \langle \alpha e^{in\omega t}|x|\beta e^{in'\omega t}\rangle \epsilon_0 \cos\omega t dt \tag{1.58}$$

The integral vanishes for $|\alpha - \beta| > 1$. The form of the Hamiltonian matrix is:

$$H_F = \begin{bmatrix} . & . & . & . & . & . & . & . & . \\ . & . & . & . & . & . & . & . & . \\ . & . & H_0+2\omega & D & 0 & 0 & 0 & . & . \\ . & . & D & H_0+\omega & D & 0 & 0 & . & . \\ . & . & 0 & D & H_0 & D & 0 & . & . \\ . & . & 0 & 0 & D & H_0-\omega & D & . & . \\ . & . & 0 & 0 & 0 & D & H_0-2\omega & . & . \\ . & . & . & . & . & . & . & . & . \\ . & . & . & . & . & . & . & . & . \end{bmatrix}$$

To set up the Floquet Hamiltonian for a KH atom, it is imperative to first define the KH Hamiltonian for a given Hamiltonian in laboratory frame:

$$\hat{H}(\vec{r},t) = -\frac{\nabla^2}{2} + V(\vec{r}) + \epsilon_0 \cos\omega t \vec{e}_z.\vec{r} \tag{1.59}$$

A well known unitary transformation[30] transforms the above Hamiltonian into the KH Hamiltonian by employing the classical variable substitution given by: $r_{KH} = r - \alpha(t)e_Z$,

$$\hat{H}(\vec{r},t) = -\frac{\nabla^2}{2} + V(r_{KH} + \alpha(t)e_Z) \tag{1.60}$$

Therefore, the Floquet Hamiltonian for the KH atom is given by:

$$\hat{H}_F(\vec{r},t) = -\frac{\nabla^2}{2} - i\frac{\partial}{\partial t} + V(r_{KH} + \alpha(t)e_Z) \tag{1.61}$$

Writing the above equation in matrix notation :

$$\begin{aligned}\langle\psi_\alpha|\hat{H}_F|\psi_\beta\rangle &= \langle\langle\sum_{n=1}^{\infty}\sum_{j=1}^{\infty} e^{-iE_\alpha t}e^{in\omega t}\phi_j(r)|\frac{\nabla^2}{2} - i\frac{\partial}{\partial t} + V(r_{KH}+\alpha(t)e_Z)| \\ &\quad \sum_{n'=1}^{\infty}\sum_{j'=1}^{\infty} e^{-iE_\beta t}e^{in'\omega t}\phi_{j'}(r)\rangle\rangle \\ &= \delta_{n,n'}H_{\alpha\beta} + \delta_{j,j'}\delta_{n,n'}n\omega + \\ &\quad \frac{1}{2\pi}\int_0^{2\pi} e^{i(n-n')\omega t}\langle\phi_j(\vec{r})|V(r_{KH}+\alpha(t)e_Z|\phi_{j'}(\vec{r})\rangle \end{aligned} \tag{1.62}$$

In the KH frame of reference, the potential $V(r_{KH}+\alpha(t)e_Z)$ is a periodic function oscillating with the frequency of laser field. Thereby, the Fourier series expansion of the potential function is taken. Therefore, substituting $V(r_{KH}+\alpha(t)e_Z) = V_0(r_{KH}) + \sum_{n=1}^{\infty} V_n(r_{KH})cos(n\omega t)$, the following matrix form is obtained for the Floquet Hamiltonian of the KH atom:

$$H_F = \begin{bmatrix} . & . & . & . & . & . & . & . & . \\ . & . & . & . & . & . & . & . & . \\ . & . & H_0^{KH}+2\omega & V_1 & V_2 & V_3 & V_4 & . & . \\ . & . & V_1 & H_0^{KH}+\omega & V_1 & V_2 & V_3 & . & . \\ . & . & V_2 & V_1 & H_0^{KH} & V_1 & V_2 & . & \\ . & . & V_3 & V_2 & V_1 & H_0^{KH}-\omega & V_1 & . & . \\ . & . & V_4 & V_3 & V_2 & V_1 & H_0^{KH}-2\omega & . & . \\ . & . & . & . & . & . & . & . & . \\ . & . & . & . & . & . & . & . & . \end{bmatrix}$$

where

$$V_n(r_{KH}) = \frac{1}{2\pi}\int_0^{2\pi} V(r_{KH}+\alpha_0 cos(\phi)e_Z)cos(n\phi)d\phi \tag{1.63}$$

The Fourier components, $V_n(r_{KH})$, are also referred to as the KH harmonics of the quantum system in super-intense laser field and are pivotal in defining the dynamics of stabilization. The zeroth-order time-independent term constitute the effective binding potential for the electron whereas the higher harmonics are responsible for its ionization. However, with sufficiently high intensity of the laser, the higher order time-dependent terms die off and therefore, only the dominating stabilizing zeroth-order potential term survives.

1.9 The (t,t′) formalism

In 1993, Peskin and Moiseyev [32] gave a novel computational method for the solution of time-dependent Schrödinger equation with time-dependent Hamiltonians. They introduced a new coordinate called t' in the time domain over which the basis of the Floquet Hamiltonian is expanded whereas the propagation of the wavepacket is carried over the t co-ordinate. The space is now constituted of a complete set of basis functions in both the space coordinate r and the time-coordinate t'. This expansion of Hilbert space allows the time-dependent Hamiltonian to be written as an infinite dimensional time-independent Hamiltonian. Therefore, the time evolution operator can then be written without requiring the time-ordering operator as chronological ordering is not required when the Hamiltonian is time-independent.

The (t, t') *formalism:* Solving the TDSE yields the following solution:[32]

$$\tilde{\psi}(x,t) = \psi(x,t',t)|_{t=t'} \tag{1.64}$$

where

$$\psi(x,t',t) = e^{-(i/\hbar)\hat{H}_F(x,t')(t-t_0)}\psi(x,t',t_0) \tag{1.65}$$

and $\hat{H}_F$(x,t′) is the Floquet-type operator

$$\hat{H}_F(x,t') = \hat{H}(x,t') - i\hbar\frac{\partial}{\partial t'} \tag{1.66}$$

In order to obtain the TDSE from Eq. [1.65], the partial derivative of ψ(x,t′,t) is taken with respect to t:

$$\begin{aligned} i\hbar\frac{\partial}{\partial t}\psi(x,t',t) &= \hat{H}_F(x,t')e^{-i\hat{H}_F(x,t')(t-t_0)/\hbar}\psi(x,t',t_0) \\ &= -i\hbar\frac{\partial}{\partial t'}\psi(x,t',t) + \hat{H}(x,t')\psi(x,t',t) \end{aligned} \tag{1.67}$$

Therefore,

$$i\hbar(\frac{\partial}{\partial t}+\frac{\partial}{\partial t'})\psi(x,t',t)=\hat{H}(x,t')\psi(x,t',t) \tag{1.68}$$

Over the contour when t = t′, we have $\frac{\partial t'}{\partial t}=1$ and therefore,

$$\frac{\partial\psi(x,t',t)}{\partial t'}|_{t'=t}+\frac{\partial\psi(x,t',t)}{\partial t}|_{t'=t}=\frac{\partial\tilde{\psi}(x,t)}{\partial t}|_{t'=t} \tag{1.69}$$

Substituting it in Eq. [1.68], the general form of TDSE is obtained:

$$i\hbar\frac{\partial\psi(x,t)}{\partial t}=\hat{H}(x,t)\psi(x,t)$$

To carry out time propagation, the initial wavepacket is expanded in the Fourier basis functions over the t' coordinate:

$$\psi(x,t',t_0)=\sum_{n=-\infty}^{\infty}e^{in\omega t'}\phi(x)$$

Now, the time evolution of the system can be evaluated such that propagation of wavepacket over n=0 Floquet channel needs to be studied only. The t' coordinate is eventually eliminated by averaging the Floquet matrix over the t' coordinate in the Fourier basis expansion.

$$\psi(x,t)=\sum_{n=-\infty}^{\infty}e^{in\omega t}[e^{-i\hat{H}_F(x)(t-t_0)}\psi(x,t_0)]_{n=0} \tag{1.70}$$

1.10 Computational Tools

The objective of the thesis is to perform quantum dynamics for time-periodic Hamiltonian by transforming it into an infinite dimensional time-independent Hamiltonian and thereby employing the computational techniques developed for solving TDSE for time-independent Hamiltonian. To carry out time propagation

of wavepackets for time-independent Hamiltonian, the split operator method is one of the simplest and most popular methods.[24]

1.10.1 The Split Operator Method

The interesting feature of the Split-operator method is that the leading order corrections scale as $\mathcal{O}(\triangle t^3)$.[24] The time evolution operator over the global time interval [0,t) is expressed as a product of propagators over a short time interval, $\triangle t$, where $N\triangle t = t$.. Thus,

$$U(t,0) = e^{-iHt/\hbar} = \underbrace{e^{-iH\triangle t/\hbar}e^{-iH\triangle t/\hbar}\ldots e^{-iH\triangle t/\hbar}}_{\text{N times}} \tag{1.71}$$

The methodology is then to split the Hamiltonian operator into kinetic and potential terms and thereby approximate each short time propagator as their product.

$$\begin{aligned} e^{-iH\triangle t\hbar} &= e^{-i(\hat{p}^2/2m+V(\hat{x}))/\triangle t/\hbar} \\ &\approx e^{-i(T\triangle t/\hbar)}e^{-i(V\triangle t/\hbar)} + \mathcal{O}(\triangle t^2) \end{aligned} \tag{1.72}$$

where T = $\hat{p}^2/2m$. The above splitting would be exact if the operators T and V commuted, otherwise an error is introduced proportional to the commutator [T,V] which is $\mathcal{O}(\triangle t^2)$. However, the leading order error term ($\sim \frac{\triangle t^2}{\hbar^2}$) can be eliminated by formulating the split such that it results in a symmetrizing product of kinetic and potential factors :

$$\begin{aligned} e^{-iH\triangle t/\hbar} &\approx e^{-i(V\triangle t/2\hbar)}e^{-i(T\triangle t/2\hbar)}e^{-i(T\triangle t/2\hbar)}e^{-i(V\triangle t/2\hbar)} \\ &= e^{-i(V\triangle t/2\hbar)}e^{-i(T\triangle t/\hbar)}e^{-i(V\triangle t/2\hbar)} + \mathcal{O}(\triangle t^3) \end{aligned} \tag{1.73}$$

Proof:

$$\begin{aligned} e^{-i(T+V)\triangle t/\hbar} &= 1 - i(T+V)\frac{\triangle t}{\hbar} + \frac{(-i)^2(T+V)^2 \triangle t^2}{2\hbar^2} + \frac{(-i)^3(T+V)^3 \triangle t^3}{3!\hbar^3} + \dots \\ &= 1 - i(T+V)\frac{\triangle t}{\hbar} - \frac{(T^2+V^2TV+VT) \triangle t^2}{2\hbar^2} \\ &+ i\frac{(T^3+TVT+T^2V+TV^2+VT^2+V^2T+VTV+V^3)}{3!\hbar^3} + \dots \end{aligned}$$

$$\begin{aligned} e^{-i(V\triangle t/2\hbar)}e^{-i(T\triangle t/\hbar)}e^{-i(V\triangle t/2\hbar)} &= \left[1 - iV\frac{\triangle t}{2\hbar} + \frac{(-iV \triangle t)^2}{8\hbar^2} + \dots\right] \times \\ &\quad \left[1 - iT\frac{\triangle t}{\hbar} + \frac{(-iT \triangle t)^2}{2\hbar^2} + \dots\right] \times \\ &\quad \left[1 - iV\frac{\triangle t}{2\hbar} + \frac{(-iV \triangle t)^2}{8\hbar^2} + \dots\right] \\ &= 1 - i(T+V)\frac{\triangle t}{\hbar} - \frac{(T^2+V^2TV+VT) \triangle t^2}{2\hbar^2} \\ &+ i(\frac{V^3}{6} + \frac{T^3}{6} + \frac{VTV}{4} + \frac{V^2T}{8} \\ &+ \frac{VT^2}{4} + \frac{T^2V}{4} + \frac{TV^2}{8})\frac{\triangle t^3}{\hbar^3} + \dots \end{aligned}$$

Comparing the above two equations, the error term of $\mathcal{O}(\triangle t^2)$ vanishes and the leading order error term corresponds to $\mathcal{O}(\triangle t^3)$:

$$\begin{aligned} Error &= i\frac{\triangle t^3}{\hbar^3}\left(\frac{T[V,T]}{12} + \frac{[T,V]T}{12} + \frac{[T,V]V}{24} + \frac{V[V,T]}{24}\right) \\ &= i\frac{\triangle t^3}{\hbar^3}\left(\frac{[T,[V,T]}{12} + \frac{[V,[V,T]}{24}\right) \end{aligned} \tag{1.74}$$

1.11 Plan of the thesis

1. The implementation of the Floquet theorem served to provide the basis for the expansion of the initial wavepacket; the (t,t′)-method is employed to carry out time-propagation of the wavepacket for time-dependent Hamiltonian (not necessarily time-periodic) by transforming it into an infinite dimensional time-independent Hamiltonian and thereby eschewing the use of time-ordering operator. However, within the (t,t′), the storage space for

the Floquet matrix of infinite order is enormous and the computational cost to calculate the propagator matrix's exponential is also huge. Therefore, a memory and time saving algorithm in length gauge was suggested by Prashant et. al. to reduce the complexity of the problem.[33] Thereby, a recursive algorithm in the (t,t′) formalism is constructed to carry out time propagation in the KH frame which is presented in Chapter 2. Also, the recursive subroutine is elaborately discussed along with the implementation scheme of the algorithm. The operation count of the algorithm is also discussed to show the effectiveness of the code.

2. In Chapter 3, the implementation of the recursive algorithm is carried out for two test cases, viz. the symmetric double well potential and the xenon model potential for the numerical validation of the proposed algorithm in the KH gauge. The wavepacket dynamics is carried out along with other modes of testing such as the convergence of the propagated wavepacket with respect to the number of Floquet channels and with time step. Further in Chapter 3, using an analogous recursive algorithm, the quantum dynamics calculation is performed for the Xenon model potential system. The complex absorbing potential methodology is also applied to absorb the artificial reflection of the wavepacket near the edges of the numerical grid. Also, time evolution of the energy expectation value of the propagated wavepacket is computed and discussed.

References

[1] M. Gavrila, *Atoms in laser fields*. Academic Press, Boston (1992).

[2] W. C. Henneberger, *Phys. Rev. Lett.* **21**, 838 (1968).

[3] M. Gavrila, *J.Phys. B: At. Mol. Opt. Phys.* **35**, R147 (2002).

[4] K. J. Meharg, J. S. Parker and K. T. Taylor, *J.Phys. B: At. Mol. Opt. Phys.* **38**, 237 (2005).

[5] A. Einstein, *Ann. Phys.* **17**, 132 (1905).

[6] A. Einstein, *Ann. Phys.* **20**, 199 (1906).

[7] M. G. Mayer, *Ann. Phys.* **9**, 273 (1931).

[8] G. S. Voronov and N. B. Delone, *JETP Letters* **1**, 66 (1965).

[9] G. S. Voronov and N. B. Delone, *Sov. Phys. JETP Letters* **23**, 54 (1966).

[10] G. Mainfray and C. Manus, *Rep. Prog. Phys.* **54**, 1333 (1991).

[11] J. H. Eberly, J. Javanainen, and K. Rzazewski, *Physics Reports* **204**, 331 (1991).

[12] J. H. Eberly and J. Javanainen, *Eur. J. Phys.* **9**, 265 (1988).

[13] M. Richter, *Imaging and Controlling Electronic and Nuclear Dynamics in Strong Laser Fields*, Ph.D. Thesis, Technischen Universität Berlin (2016).

[14] L. V. Keldysh, *Sov. Phys. JETP* **20**, 1307 (1965).

[15] F. H. M. Faisal, *Theory of Multiphoton Processes*, Springer, Boston, MA.

[16] C. Joachain, N. Kylstra, and R. Potvliege, *Atoms in Intense Laser Fields*, Cambridge: Cambridge University Press (2011).

[17] M. Y. Ivanov, M. Spanner, and O. Smirnova, *J. Mod. Opt.* **52**, 165 (2005).

[18] M. Gavrila and J. Z. Kaminski, *Phys. Rev. Lett.* **52**, 614 (1984).

[19] J. I. Gersten and M. H. Mittleman, *J. Phys. B* **9**, 2561 (1976).

[20] H. A. Kramers, *Collected Scientific Papers* (North-Holland, Amsterdam, 1956). W. C. Henneberger, *Phys. Rev. Lett.* **21**, 838 (1968).

[21] W. Pauli and M. Fierz, *Nuovo Cimento* **15**, 167 (1938).

[22] J. H. Eberly and K. C. Kulander, *Science* **262**, 1229 (1993).

[23] F. Morales, M. Richter, S. Patchkovskii and O. Smirnova, *Proc. Natl. Acad. Sci.* **108**, 16906 (2011).

[24] David J. Tannor, *Introduction to Quantum Mechanics: A Time-Dependent Perspective.* Sausalito, Calif: University Science Books (2007).

[25] C. Leforestier, R. H. Bisseling, C. Cerjan, D. Feit, R. Friesner, A. Guldberg, A. Hammerich, G. Jolicard, W. Karrlein, H. D. Meyer, N. Lipkin, O. Roncero and R. Kosloff, *J. Comp. Phys.* **94**, 59 (1991).

[26] D. Kosloff and R. Kosloff, *J. Comput. Phys.* **52**, 35 (1983).

[27] M. D. Feit, J. A. Fleck Jr. and A. Steiger, *J. Comput. Phys.* **47**, 412 (1982).

[28] H. T.-Ezer and R. Kosloff, *J. Chem. Phys.* **81**, 3967 (1984).

[29] C. Joachain, N. Kylstra and R. Potvliege, *Atoms in Intense Laser Fields.* Cambridge: Cambridge University Press (2011).

[30] M. Pont, M. Gavrila *Phys. Rev. Lett.* **65**, 2362 (1990).

[31] J. H. Shirley, *Phys. Rev.* **138**, B979 (1965).

[32] U. Peskin and N. Moiseyev, *J. Chem. Phys.* **99**, 4590 (1993).

[33] P. Raj, A. Gugalia and P. Balanarayan, *to be published.*

Chapter 2

A Recursive Algorithm in (t,t′) for quantum dynamics in the Kramers-Henneberger frame

2.1 A Memory and Time Saving Algorithm for (t,t′) method in length gauge

The algorithm presented here is the work by Prashant et al.[1] Considering a quantum system in an oscillating electric field linearly polarized along the z direction such that the Hamiltonian of the system is (in a.u.): $\hat{H} = -\frac{\nabla^2}{2} + V(\vec{r}) + \varepsilon_0 \hat{e}_z.\vec{r}\cos\omega t$, where V($\vec{r}$) is the time-independent potential and $\varepsilon_0 \hat{e}_z.\vec{r}\cos\omega t$ is the time-dependent electric field component. The TDSE for such a system is given as:

$$i\frac{\partial\psi(\vec{r},t)}{\partial t} = \left[-\frac{\hat{\nabla}^2}{2} + V(\vec{r}) + \varepsilon_0.\hat{e}_z\vec{r}\cos\omega t \right]\psi(\vec{r},t) \tag{2.1}$$

The Floquet Hamiltonian for such a system from Eq. [1.55] is then:

$$\hat{H}_f = -\frac{\hat{\nabla}^2}{2} + V(\vec{r}) - i\frac{\partial}{\partial t} + \varepsilon_0\hat{e}_z.\vec{r}\cos\omega t \tag{2.2}$$

Let $\hat{H}_0 = -\frac{\hat{\nabla}^2}{2} + V(\vec{r})$ and $D = \frac{\varepsilon_0 \hat{e}_z.\vec{r}}{2}$ be the dipole term. Therefore, from Eq. [1.56], the Floquet Hamiltonian in block tridiagonal form [2] for n Floquet channels is represented as:

$$[H_f] = [H_0 + n\omega]_{n,n'} + [D]_{n,n'\pm 1} \tag{2.3}$$

In an expanded form the Floquet matrix has the form (here, for 2 Floquet channels):

$$[H_f] = \begin{bmatrix} [H_0+2\omega] & [D] & 0 & 0 & 0 \\ [D] & [H_0+\omega] & [D] & 0 & 0 \\ 0 & [D] & [H_0] & [D] & 0 \\ 0 & 0 & [D] & [H_0-\omega] & [D] \\ 0 & 0 & 0 & [D] & [H_0-2\omega] \end{bmatrix}_{(n_f\times n_x, n_f\times n_x)}$$

Here, n_f is the number of Floquet channels and n_x is the numerical grid size. Once the Floquet Hamiltonian matrix is constructed, the following steps are involved in the proposed memory and time saving algorithm for time-propagation of the wavepacket:

Step 1: $[H_f] = [H_D] + [H_{num}]$; this involves a separation of the number matrix giving [H_D] a uniform block tridiagonal form.

$$[H_f] = \begin{bmatrix} [H_0] & [D] & 0 & 0 & 0 \\ [D] & [H_0] & [D] & 0 & 0 \\ 0 & [D] & [H_0] & [D] & 0 \\ 0 & 0 & [D] & [H_0] & [D] \\ 0 & 0 & 0 & [D] & [H_0] \end{bmatrix} + \begin{bmatrix} [2\omega][\mathbf{I}] & 0 & 0 & 0 & 0 \\ 0 & [\omega][\mathbf{I}] & 0 & 0 & 0 \\ 0 & 0 & 0 & 0 & 0 \\ 0 & 0 & 0 & [-\omega][\mathbf{I}] & 0 \\ 0 & 0 & 0 & 0 & [-2\omega][\mathbf{I}] \end{bmatrix}$$

Step 2: The symmetry of the [H_D] matrix is used to analytically block-diagonalize it using Chebyshev polynomials of the second kind. [3] Therefore, $H_D = U^\dagger H_d U$, where H_d in the block diagonal form is: [H_0] + $\vec{r}.\vec{\epsilon}\,\delta_{nn'}$.

$$[H_d] = \begin{bmatrix} [H_0 + \vec{r}.\vec{\epsilon}\cos(\tau_1)] & 0 & 0 & 0 & 0 \\ 0 & [H_0 + \vec{r}.\vec{\epsilon}\cos(\tau_2)] & 0 & 0 & 0 \\ 0 & 0 & [H_0 + \vec{r}.\vec{\epsilon}\cos(\tau_3)] & 0 & 0 \\ 0 & 0 & 0 & [H_0 + \vec{r}.\vec{\epsilon}\cos(\tau_4)] & 0 \\ 0 & 0 & 0 & 0 & [H_0 + \vec{r}.\vec{\epsilon}\cos(\tau_5)] \end{bmatrix}$$

where $\tau_k = \frac{k\pi}{n_f+1}$. The unitary matrix form of stacked up eigenvectors is:

$$U_{ij} = \sqrt{\frac{2}{n_f+1}} \sin(i\tau_j) \tag{2.4}$$

Here i index runs from 1 to $2 * n_f + 1$ (n_f is the number of Floquet channels.) This effectively reduces the storage space to $(n_x \times n_x)$ order matrices, where n_x is the grid size in the spatial representation of $\hat{H}_0$, which is the physical field-free Hamiltonian. The unitary matrix over the full Floquet dimensions is constructed as: (n_f=2 here shown as an example.)

$$[U] = \begin{bmatrix} U_{11}[I] & U_{12}[I] & U_{13}[I] & U_{14}[I] & U_{15}[I] \\ U_{21}[I] & U_{22}[I] & U_{23}[I] & U_{24}[I] & U_{25}[I] \\ U_{31}[I] & U_{32}[I] & U_{33}[I] & U_{34}[I] & U_{35}[I] \\ U_{41}[I] & U_{42}[I] & U_{43}[I] & U_{44}[I] & U_{45}[I] \\ U_{51}[I] & U_{52}[I] & U_{53}[I] & U_{54}[I] & U_{55}[I] \end{bmatrix}$$

where [I] is the identity matrix with dimensions $(n_x \times n_x)$. This unitary matrix need not be constructed or stored at all in the algorithm. It can be generated as and when required because of its analytical form.

Step 3: The next step is to calculate the propagator. Since H_D and H_{num} do not commute so the propagator operator is calculated by employing the split. [4] Thus,

$$\begin{aligned} e^{-iH_f t} &= e^{-i(H_D+H_{num})t} \\ e^{-iH_f t} &= e^{-iH_{num}t/2} e^{iUH_d U^\dagger t} e^{-iH_{num}t/2} \\ e^{-iH_f t} &= e^{-iH_{num}t/2} U e^{iH_d t} U^\dagger e^{-iH_{num}t/2} \end{aligned} \tag{2.5}$$

Full Algorithm: By the (t,t′) formalism, the propagation of wavepacket corresponding to the zeroth Floquet channel needs to studied only. The physical solution, $\psi(\vec{r}, t)$ is then obtained from the full solution $\psi(\vec{r}, t, t')$ by setting t=t′. The time propagation of an initial wavepacket $\psi(\vec{r}, t_0)_n$, by employing the proposed memory and time saving algorithm with one Floquet channel, is carried out

as follows:

$$\psi(\vec{r},t) = e^{\frac{-in\omega\triangle t}{2}} U \begin{bmatrix} e^{-i(H_d)_1\triangle t} & 0 & 0 \\ 0 & e^{-i(H_d)_2\triangle t} & 0 \\ 0 & 0 & e^{-i(H_d)_3\triangle t} \end{bmatrix} U^{\dagger} e^{-\frac{in\omega\triangle t}{2}} (\psi(\vec{r},t_0)_n)$$

Following the (t,t′) formalism [5] of time propagation, when using the Floquet basis, the exponential of the Floquet matrix needs to be evaluated which amounts to being computationally very expensive along with huge storage space. Therefore, the proposed memory and time saving algorithm is employed to solve the TDSE within the (t,t′) framework as the number of operations is drastically reduced in the current scheme.

2.2 Quantum Dynamics in the Kramers-Henneberger Frame

The time propagation of an initial state $\psi(r;t)$ is carried forth using a propagator operator:

$$\psi(r;t) = \hat{U}(t;t_0)\psi(r;t_0) \tag{2.6}$$

Here, $\hat{U}(t;t_0)$ is the propagator operator [6] given by:

$$\hat{U}(t;t_0) = e^{-\frac{i}{\hbar}\int_{t_0}^{t} \hat{H}_F dt} \tag{2.7}$$

The unitary transformation of the TDSE from the length gauge to the KH gauge yields a time-periodic potential, $V(\vec{r}_{KH}+\alpha(t)e_z)$, whose KH harmonics are given by:

$$V(\vec{r}_{KH} + \alpha(t)e_Z) = V_0(\vec{r}_{KH}) + \sum_{n=1}^{\infty} V_n(\vec{r}_{KH})cos(n\omega t) \tag{2.8}$$

Once the harmonics of the potential in the KH frame are generated, the time propagator operator can then be constructed by block-diagonalizing the Floquet Hamiltonian at each time step and compute the propagator using the split:

$$\hat{U}(t,0) = e^{-i\hat{H}t/\hbar} = \underbrace{e^{-i\hat{H}\triangle t/\hbar}e^{-i\hat{H}\triangle t/\hbar}\ldots e^{-i\hat{H}\triangle t/\hbar}}_{\text{N times}} \tag{2.9}$$

Since the complexity of the diagonalization of a matrix is of the order of $\mathcal{O}(N^3)$ so this computation will be very expensive as it involves the diagonalization of the Floquet matrix whose dimensions are $[(n_x{}^*f_{ch})\times(n_x{}^*f_{ch})]$, where n_x = the number of grid points on x, and $fch = 2^*\mathrm{n}_f{+}1$ where n_f is the number of Floquet channels. Hence, the memory and time saving algorithm for the (t,t′) method is employed in the KH frame to efficaciously calculate the propagator operator and carry out the time propagation. The algorithm is constructed in a recursive manner so that it is valid for any number of KH harmonics and Floquet channels.

2.2.1 The Recursive Algorithm in the Kramers-Henneberger Frame

For two Floquet channels and five KH harmonics, the Floquet Hamiltonian in the Kramers-Henneberger frame of reference is:

$$[H_F] = \begin{bmatrix} [H_0^{KH}+2\omega] & [V_1^{KH}] & [V_2^{KH}] & [V_3^{KH}] & [V_4^{KH}] \\ [V_1^{KH}] & [H_0^{KH}+\omega] & [V_1^{KH}] & [V_2^{KH}] & [V_3^{KH}] \\ [V_2^{KH}] & [V_1^{KH}] & [H_0^{KH}] & [V_1^{KH}] & [V_2^{KH}] \\ [V_3^{KH}] & [V_2^{KH}] & [V_1^{KH}] & [H_0^{KH}-\omega] & [V_1^{KH}] \\ [V_4^{KH}] & [V_3^{KH}] & [V_2^{KH}] & [V_1^{KH}] & [H_0^{KH}-2\omega] \end{bmatrix}$$

$$\langle\psi_\alpha|\hat{H}_F|\psi_\beta\rangle = \delta_{n,n'}H_0^{KH} + \delta_{j,j'}\delta_{n,n'}n\omega + \delta_{j,j'}\delta_{n,n'\pm n}V_n^{KH}(\vec{r}_{KH})$$

$$V_n(r_{KH}) = \tfrac{1}{2\pi}\int_0^{2\pi} V(r_{KH}+\alpha_0 cos(\omega t)e_Z)cos(n\omega t)dt \;;\; H_0^{KH} = -\tfrac{\nabla^2}{2} + V_0^{KH}$$

Step 1: Separation of the number matrix and the Fourier components:

$$[H_F] = \begin{bmatrix} [H_0^{KH}] & 0 & 0 & 0 & 0 \\ 0 & [H_0^{KH}] & 0 & 0 & 0 \\ 0 & 0 & [H_0^{KH}] & 0 & 0 \\ 0 & 0 & 0 & [H_0]^{KH} & 0 \\ 0 & 0 & 0 & 0 & [H_0^{KH}] \end{bmatrix} + \begin{bmatrix} 0 & [V_1^{KH}] & 0 & 0 & 0 \\ [V_1^{KH}] & 0 & [V_1^{KH}] & 0 & 0 \\ 0 & [V_1^{KH}] & 0 & [V_1^{KH}] & 0 \\ 0 & 0 & [V_1^{KH}] & 0 & [V_1^{KH}] \\ 0 & 0 & 0 & [V_1^{KH}] & 0 \end{bmatrix}$$

$$+ \begin{bmatrix} 0 & 0 & [V_2^{KH}] & 0 & 0 \\ 0 & 0 & 0 & [V_2^{KH}] & 0 \\ [V_2^{KH}] & 0 & 0 & 0 & [V_2^{KH}] \\ 0 & [V_2^{KH}] & 0 & 0 & 0 \\ 0 & 0 & [V_2^{KH}] & 0 & 0 \end{bmatrix} + \begin{bmatrix} 0 & 0 & 0 & [V_3^{KH}] & 0 \\ 0 & 0 & 0 & 0 & [V_3^{KH}] \\ 0 & 0 & 0 & 0 & 0 \\ [V_3^{KH}] & 0 & 0 & 0 & 0 \\ 0 & [V_3^{KH}] & 0 & 0 & 0 \end{bmatrix}$$

$$+ \begin{bmatrix} 0 & 0 & 0 & 0 & [V_4^{KH}] \\ 0 & 0 & 0 & 0 & 0 \\ 0 & 0 & 0 & 0 & 0 \\ 0 & 0 & 0 & 0 & 0 \\ [V_4^{KH}] & 0 & 0 & 0 & 0 \end{bmatrix} + \begin{bmatrix} [2\omega][\mathbf{I}] & 0 & 0 & 0 & 0 \\ 0 & [\omega][\mathbf{I}] & 0 & 0 & 0 \\ 0 & 0 & 0 & 0 & 0 \\ 0 & 0 & 0 & [-\omega][\mathbf{I}] & 0 \\ 0 & 0 & 0 & 0 & [-2\omega][\mathbf{I}] \end{bmatrix}$$

Step 2: After the separation of the number matrix and the matrices of the Fourier components from the Floquet matrix, the next step is carry out analytical block-diagonalization of the matrices of KH harmonics. This is carried out in the following way:

Consider the matrix of first KH harmonic which needs to be diagonalized:

$$V_1^{KH} = \begin{bmatrix} 0 & [V_1^{KH}] & 0 & 0 & 0 \\ [V_1^{KH}] & 0 & [V_1^{KH}] & 0 & 0 \\ 0 & [V_1^{KH}] & 0 & [V_1^{KH}] & 0 \\ 0 & 0 & [V_1^{KH}] & 0 & [V_1^{KH}] \\ 0 & 0 & 0 & [V_1^{KH}] & 0 \end{bmatrix}_{[(2n_f+1)*n_x,(2n_f+1)*n_x]}$$

Diagonalization of the above matrix is performed by using the eigenvalues and eigenvectors of the following matrix:

$$\begin{bmatrix} 0 & 1 & 0 & 0 & 0 \\ 1 & 0 & 1 & 0 & 0 \\ 0 & 1 & 0 & 1 & 0 \\ 0 & 0 & 1 & 0 & 1 \\ 0 & 0 & 0 & 1 & 0 \end{bmatrix}_{[2n_f+1,2n_f+1]}$$

Let $a_i^1 (i = 1, 2, \ldots, 2 * n_f + 1)$ be the eigenvalues and U_1 be the eigenvector matrix of the above matrix. Then, the block-diagonalization of the V_1^{KH} is simply:

$$V_1^d = \begin{bmatrix} [V_1^{KH} * a_1^1] & 0 & 0 & 0 & 0 \\ 0 & [V_1^{KH} * a_2^1] & 0 & 0 & 0 \\ 0 & 0 & [V_1^{KH} * a_3^1] & 0 & 0 \\ 0 & 0 & 0 & [V_1^{KH} * a_4^1] & 0 \\ 0 & 0 & 0 & 0 & [V_1^{KH} * a_5^1] \end{bmatrix}_{[(2n_f+1)*n_x,(2n_f+1)*n_x]}$$

In the diagonal form, the exponential of a matrix is just the exponential of its eigenvalues. And, $V_1^{KH} = U_1 V_1^d U_1^\dagger$. Therefore, the computation of diagonalizing the matrix of dimensions $[(2n_f + 1) * n_x, (2n_f + 1) * n_x]$ is avoided by performing the above analytical block-diagonalization.

Step 3: To evaluate the propagator operator, the exponential of the Floquet Hamiltonian is carried out using the split operator approximation [9] in the following way:

$$e^{-iH_F \triangle t} = e^{-\frac{iH_{num}\triangle t}{2}} U_4 e^{-\frac{iV_4^{KH}\triangle t}{2}} U_4^\dagger U_3 e^{-\frac{iV_3^{KH}\triangle t}{2}} U_3^\dagger U_2 e^{-\frac{iV_2^{KH}\triangle t}{2}} U_2^\dagger U_1 e^{-\frac{iV_1^{KH}\triangle t}{2}} U_1^\dagger$$
$$U_0 e^{-iH_0^{KH}\triangle t} U_0^\dagger U_1 e^{-\frac{iV_1^{KH}\triangle t}{2}} U_1^\dagger U_2 e^{-\frac{iV_2^{KH}\triangle t}{2}} U_2^\dagger U_3 e^{-\frac{iV_3^{KH}\triangle t}{2}} U_3^\dagger U_4 e^{-\frac{iV_4^{KH}\triangle t}{2}} U_4^\dagger e^{-\frac{iH_{num}\triangle t}{2}} \quad (2.10)$$

Here, $\hat{U}_1$, $\hat{U}_2$, $\hat{U}_3$, $\hat{U}_4$ are the eigenvectors which are used for block-diagonalizing the exponential of the KH harmonic matrices. The eigenvalues and eigenvectors for block-diagonalization along with the general diagonalization scheme is given in Appendix 1.

Step 4: If $\psi(\vec{r},t_0)$ is the initial wavepacket then the full algorithm to carry out time propagation is given by:

$$\psi(\vec{r},t)=\begin{bmatrix}\begin{bmatrix}e^{-\frac{i(2\omega)\triangle t}{2}}\end{bmatrix}\\\begin{bmatrix}e^{-\frac{i(\omega)\triangle t}{2}}\end{bmatrix}\\0\\\begin{bmatrix}e^{-\frac{i(-\omega)\triangle t}{2}}\end{bmatrix}\\\begin{bmatrix}e^{-\frac{i(-2\omega)\triangle t}{2}}\end{bmatrix}\end{bmatrix}U_4\begin{bmatrix}[e^{-(iV_4^{d^i}\triangle t)/2}]\\[e^{-(iV_4^{d^{ii}}\triangle t)/2}]\\[e^{-(iV_4^{d^{iii}}\triangle t)/2}]\\[e^{-(iV_4^{d^{iv}}\triangle t)/2}]\\[e^{-(iV_4^{d^{v}}\triangle t)/2}]\end{bmatrix}U_4^\dagger U_3\begin{bmatrix}[e^{-(iV_3^{d^i}\triangle t)/2}]\\[e^{-(iV_3^{d^{ii}}\triangle t)/2}]\\[e^{-(iV_3^{d^{iii}}\triangle t)/2}]\\[e^{-(iV_3^{d^{iv}}\triangle t)/2}]\\[e^{-(iV_3^{d^{v}}\triangle t)/2}]\end{bmatrix}U_3^\dagger U_2\begin{bmatrix}[e^{-(iV_2^{d^i}\triangle t)/2}]\\[e^{-(iV_2^{d^{ii}}\triangle t)/2}]\\[e^{-(iV_2^{d^{iii}}\triangle t)/2}]\\[e^{-(iV_2^{d^{iv}}\triangle t)/2}]\\[e^{-(iV_2^{d^{v}}\triangle t)/2}]\end{bmatrix}U_2^\dagger U_1\ldots$$

$$\begin{bmatrix}[e^{-(iV_1^{d^i}\triangle t)/2}]\\[e^{-(iV_1^{d^{ii}}\triangle t)/2}]\\[e^{-(iV_1^{d^{iii}}\triangle t)/2}]\\[e^{-(iV_1^{d^{iv}}\triangle t)/2}]\\[e^{-(iV_1^{d^{v}}\triangle t)/2}]\end{bmatrix}U_1^\dagger U_0\begin{bmatrix}[e^{-i(H_0^{KH})\triangle t}]\\[e^{-i(H_0^{KH})\triangle t}]\\[e^{-i(H_0^{KH})\triangle t}]\\[e^{-i(H_0^{KH})\triangle t}]\\[e^{-i(H_0^{KH})\triangle t}]\end{bmatrix}U_0^\dagger U_1\begin{bmatrix}[e^{-(iV_1^{d^i}\triangle t)/2}]\\[e^{-(iV_1^{d^{ii}}\triangle t)/2}]\\[e^{-(iV_1^{d^{iii}}\triangle t)/2}]\\[e^{-(iV_1^{d^{iv}}\triangle t)/2}]\\[e^{-(iV_1^{d^{v}}\triangle t)/2}]\end{bmatrix}U_1^\dagger U_2\begin{bmatrix}[e^{-(iV_2^{d^i}\triangle t)/2}]\\[e^{-(iV_2^{d^{ii}}\triangle t)/2}]\\[e^{-(iV_2^{d^{iii}}\triangle t)/2}]\\[e^{-(iV_2^{d^{iv}}\triangle t)/2}]\\[e^{-(iV_2^{d^{v}}\triangle t)/2}]\end{bmatrix}U_2^\dagger U_3\ldots$$

$$\begin{bmatrix}[e^{-(iV_3^{d^i}\triangle t)/2}]\\[e^{-(iV_3^{d^{ii}}\triangle t)/2}]\\[e^{-(iV_3^{d^{iii}}\triangle t)/2}]\\[e^{-(iV_3^{d^{iv}}\triangle t)/2}]\\[e^{-(iV_3^{d^{v}}\triangle t)/2}]\end{bmatrix}U_3^\dagger U_4\begin{bmatrix}[e^{-(iV_4^{d^i}\triangle t)/2}]\\[e^{-(iV_4^{d^{ii}}\triangle t)/2}]\\[e^{-(iV_4^{d^{iii}}\triangle t)/2}]\\[e^{-(iV_4^{d^{iv}}\triangle t)/2}]\\[e^{-(iV_4^{d^{v}}\triangle t)/2}]\end{bmatrix}U_4^\dagger\begin{bmatrix}\begin{bmatrix}e^{-\frac{i(2\omega)\triangle t}{2}}\end{bmatrix}\\\begin{bmatrix}e^{-\frac{i(\omega)\triangle t}{2}}\end{bmatrix}\\0\\\begin{bmatrix}e^{-\frac{i(-\omega)\triangle t}{2}}\end{bmatrix}\\\begin{bmatrix}e^{-\frac{i(-2\omega)\triangle t}{2}}\end{bmatrix}\end{bmatrix}\psi(\vec{r},t_0)$$

The implementation of the above algorithm is done recursively so that the code works for any potential, provided the Fourier components of the potential are calculated externally and fed into the recursive subroutine as an input. The recursive subroutine also reduces the size of the code substantially.

2.3 Code Description

The complete code is provided in Appendix 2. The key sections of the code and the recursive subroutine are elaborately described in the forthcoming sections.

CODE SCHEME

1: LIBRARIES USED: **LAPACK [7], BLAS**
2: Input:
3: **T** ← Kinetic energy matrix constructed from Fourier grid Hamiltonian method.
4: **V** ← The KH harmonics matrix of the potential. The expression for the Fourier components of potential is evaluated using Wolfram Mathematica [8].
5: $\mathbf{H_0}$ ← Kinetic energy and zeroth KH component matrix.
6: **V_eval**, **V_U** ← Eigenvalues and eigenvector matrices for analytical diagonalization.
7: **fch, fld, omega, alpha, Nf** ← Floquet variables.
8: **evec_fl** ← Initial wavepacket.
9: Output:
10: **psi** ← Propagated wavepacket.
11: **nrm** ← Norm of the propagated wavepacket.
12: Subroutines:
13: **recur1** ← Recursive subroutine to evaluate right half of the split expression in eqn (2.6) ahead of $U_0 e^{-iH_0^{KH}\Delta t} U_0^\dagger$.
14: **recur2** ← Recursive subroutine to evaluate left half of the split expression in eqn (2.6) before $U_0 e^{-iH_0^{KH}\Delta t} U_0^\dagger$.
15: **DSYEV_WT_EIGVECS** ← Subroutine to diagonalize a real matrix using LAPACK library.

The schematic description of the code consists of the following key segments. The initial section of the code comprises of defining the kinetic energy matrix, the KH harmonics matrix and the initial wavepacket along with all the variables that is used for time propagation. Two recursive subroutines *recur1* and *recur2* are constructed that are responsible for the analytical block-diagonalization of the KH harmonic matrices and evaluation of the split. In both these subroutines, the operations that are performed correspond to matrix vector multiplication. Also, LAPACK and BLAS libraries are used for the diagonalization of matrices when required. In the following section, the recursive subroutine is presented along with the flowchart of the algorithm which effectively describes its implementation to carry out time propagation in the KH gauge.

THE RECURSIVE SUBROUTINE

1: **do** i ← 1 to fch
2: **do** j ← 1 to fch
3: U_j(i,j)=V_U((N-1)*fch+i,(N-1)*fch+j) ← Analytical block-diagonalization.
4: **enddo**
5: **enddo**
6: U_jt = transpose(U_j)
7: **do** j ← 1 to fch
8: **do** i ← 1 to num
9: s = (0.0d0,0.0d0)
10: **do** k ← 1 to fch
11: s = s + (U_jt(j,k)*P_fl((k-1)*num+i)) ← ***Operation count = num*fch***^{2}
12: **enddo**
13: PU((j-1)*num+i) = s ← $\mathbf{PU = U_n^\dagger \psi(x,t)}$
14: **enddo**
15: **enddo**
16: **do** i ← 1 to fch — Construction of $\mathbf{e^{-iV_n^{KH}\Delta t}/2}$ matrix.
17: **do** j ← 1 to num
18: V_exp((i-1)*num+j,(i-1)*num+j) = exp(-0.5d0*ci*dt*(V(j,N+1)*
19: V_eval((N-1)*fch+i))) ← ***Operation count = num*fch***
20: **enddo**
21: **enddo**
22: PV(:) = V_exp(:) * PU(:) ← $\mathbf{PV = e^{-iV_n^{KH}\Delta t/2} * U_n^\dagger \psi(x,t)}$
23: PU2 = (0.0d0,0.0d0)
24: **do** i ← 1 to fch
25: **do** j ← 1 to num
26: s = (0.0d0,0.0d0)
27: **do** k ← 1 to fch
28: s = s + (U j(j,k) * PV((k-1)*num+i)) ← ***Operation count = num*fch***^{2}
29: **enddo**
30: PU2((j-1)*num+i) = s
31: **enddo**
32: **enddo**
33: P_fl = PU2 ← $\mathbf{P\_fl = U_n * e^{-iV_n^{KH}\Delta t/2} * U_n^\dagger \psi(x,t)}$

34: **if** (N $\geq$ 2) **then**

35: call recur1(P_fl, N-1, fch, fch, fld, num, V_U, V_eval, V, dt) $\leftarrow$ **The Recursion**

36: **endif**

The analytical block-diagonalization of the exponential of the KH harmonic matrices is performed using the above recursive subroutine. The mathematical flow that is maintained throughout the subroutine is that of a matrix vector multiplication. Also, the time propagation algorithm is implemented in such a fashion that multiplication with zeroes of the sparse matrices is avoided so that it does not account for more operations.

As shown in the recursive algorithm flowchart in [Fig.2.1], the subroutine *recur1* is called until N=1, following which the program flow goes to the main body of the code where $e^{-iH_0^{KH}\Delta t}\psi^*(x,t)$ is evaluated which is followed by calling the recursive subroutine *recur2* which evaluates the rest of terms of the split. ($\psi^*(x,t)$ is the wavepacket obtained upon the action of *recur1*.)

```
if ( N ≥ 2 ) then
call recur1( P_fl, N-1, fch, fch, fld, num, V_U, V_eval, V, dt )
endif
```

The Recursion: The concluding section of the recursive subroutine accounts for the recursion. As can be seen in the above snippet of the code, the value of N gets updated each time the recursive subroutine is called. Consider again the dynamics for 2 Floquet channels for which N=5. With update in the value of N, the unitary matrices, which are used for analytical block-diagonalization, also gets updated and thereby, using those matrices, the exponential of the KH harmonic matrix is constructed for the corresponding value of N. The following snippet explains the recursion in a precise way:

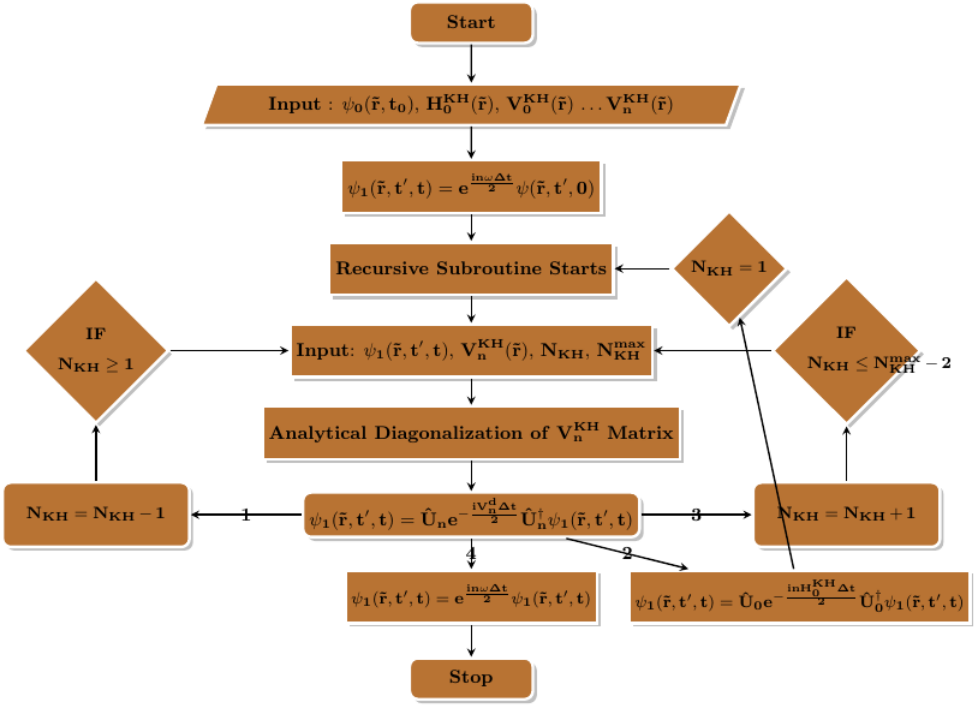

FIGURE 2.1: The dynamics algorithm flowchart: the time propagation scheme is implemented in a recursive manner. The separation of the number matrix and all the KH harmonic matrices is done initially following which the flow transfers to the recursive subroutine where analytical block-diagonalization and split is evaluated. This is performed at each time step till propagation needs to be carried out.

Recursion 1: $\psi_4(\vec{r},t) = \hat{U}_4 e^{-iV_4^{KH}\Delta t/2}\hat{U}_4^\dagger \psi_i(\vec{r},t)$

Recursion 2: $\psi_3(\vec{r},t) = \hat{U}_3 e^{-iV_3^{KH}\Delta t/2}\hat{U}_3^\dagger \psi_4(\vec{r},t)$

Recursion 3: $\psi_2(\vec{r},t) = \hat{U}_2 e^{-iV_2^{KH}\Delta t/2}\hat{U}_2^\dagger \psi_3(\vec{r},t)$

Recursion 4: $\psi_1(\vec{r},t) = \hat{U}_1 e^{-iV_1^{KH}\Delta t/2}\hat{U}_1^\dagger \psi_2(\vec{r},t)$

The most interesting feature of the recursion is that it can be called any number of times, i.e., the algorithm is valid for any number of Fourier components of the KH potential. Therefore, the systems whose Fourier components are not analytically calculable can have infinite number of numerically calculated components and so, the recursive subroutine can then be easily implemented to carry out time propagation in the KH gauge without being computationally expensive.

2.3.1 Operation Count

The operation count for the implementation of the Split-operator method into the algorithm is given as:

1. $e^{-\frac{iH_{num}\triangle t}{2}}$ in the matrix form is a diagonal matrix. So, the evaluation of $e^{-\frac{iH_{num}\triangle t}{2}}\psi(x,t)$ requires the following number of operations: *(fch*num)*, where fch = 2*Nf+1 and num is the grid size.

2. Each time the recursive subroutine is called, it evaluates $U_n e^{-\frac{iV_1^{KH}\triangle t}{2}} U_n^\dagger \psi^*(x,t)$ for which the operation count is (num*fch^2 + fch + num*fch^2). Therefore, the total operation count for Nf number of Floquet channels is: *2(fch-1)*(2*num*fch^2 + fch)*

3. For the evaluation of $U_0 e^{-iH_0^{KH}\triangle t} U_0^\dagger \psi^*(x,t)$ the number of operations which are required is: *(fch*num^2 + fch^2*num^2)*

4. The total operation count in each time step to carry out wavepacket dynamics by employing the recursive algorithm is: *num^2*(fch^2 + fch) + num*(4*fch^3 - 4*fch^2 + fch) + 2*fch(fch-1)* $\approx \mathcal{O}(num^2)$

Hence, the current time propagation scheme in the KH gauge scales to $\mathcal{O}(num^2)$ which saves a lot of computational cost for studying time evolution of a quantum system in the presence of laser. In the following chapter, the recursive algorithm is tested and validated to carry out quantum dynamics for two test cases: the symmetric double well potential and the xenon model potential.

References

[1] P. Raj, A. Gugalia and P. Balanarayan, *to be published.*

[2] J.H. Shirley, *Physical Review* **138**, B979 (1965).

[3] S. Chu, *J. Chem. Phys.* **75**, 2215 (1981).

[4] David J. Tannor, *Introduction to Quantum Mechanics: A Time-Dependent Perspective.* Sausalito, Calif: University Science Books (2007).

[5] U. Peskin and N. Moiseyev, *J. Chem. Phys.* **99**, 4590 (1993).

[6] C. Leforestier, R. H. Bisseling, C. Cerjan, D. Feit, R. Friesner, A. Guldberg, A. Hammerich, G. Jolicard, W. Karrlein, H. D. Meyer, N. Lipkin, O. Roncero and R. Kosloff, *J. Comp. Phys.* **94**, 59 (1991).

[7] E. Anderson, Z. Bai, C. Bischof, S. Blackford, J. Demmel, J. Dongarra, J. Du Croz, A. Greenbaum, S. Hammarling, A. McKenney, and D. Sorensen, *LAPACK Users' Guide*, Third edition, Society for Industrial and Applied Mathematics, 1999.

[8] Wolfram Research, Inc., *Mathematica*, Version 11.3, Champaign, IL, (2018).

Chapter 3

Numerical Validation and Testing

The model potentials chosen for the validation and testing of the recursive algorithm in (t,t′) in the KH gauge are the symmetric double well and the xenon model potential. The wavepacket dynamics is carried out along with other modes of testing like convergence over the number of Floquet channels and time steps, conservation of norm, etc. The time-independent KH calculation is performed for both systems and the expected result is verified with the wavepacket dynamics calculation.

3.1 Case 1: Symmetric Double Well Potential: Ax^4 - Bx^2

The last few decades have witnessed immense research interests in understanding the detailed dynamics of quantum systems that are exposed to strong time-dependent external fields. One such quantum system is the double well potentials which are associated with the prototype model of coherence effect, namely quantum tunneling. [1–4] The double-well potentials have also been extensively studied for various other systems such as proton transfer in DNA, [5] inversion doubling in ammonia, [6] hydrogen bonding, [7] etc.

The symmetric double well potential chosen for the test calculation is of the form

$\mathrm{Ax}^4 - Bx^2$, where A = 0.0052248 and B = 0.0139753 in atomic units. The parameters chosen correspond to the double well potential of the umbrella type inversion of ammonia molecule. Following the KH transformation, the first task at hand is to evaluate the harmonics of the KH potential. Substituting $\mathrm{x}_{KH} = x - \alpha(t)e_Z$, the form of the model potential transforms to $V(\mathrm{x}) = A(x - \alpha\cos\omega t)^4 - B(x - \alpha\cos\omega t)^2$. Now, the KH harmonics are evaluated as: $V_n(x_{KH}) = \frac{1}{2\pi}\int_0^{2\pi} V(x_{KH} + \alpha_0 cos(\omega t)e_Z)cos(n\omega t)dt$. The Wolfram Mathematica [8] computing system is utilized for calculating the integrals i.e. the harmonics of the KH potential depicted in [Fig.3.1], given by:

$$
\begin{aligned}
V_0(x) &= \frac{1}{2\pi}\int_0^{2\pi} A(x-\alpha\cos\phi)^4 - B(x-\alpha\cos\phi)^2 d\phi \\
&= \frac{1}{2}\pi(-B\pi(\alpha^2+2x^2) + A(\frac{3\alpha^4\pi}{4} + 6\alpha^2\pi x^2 + 2\pi x^4) && (3.1)\\
V_1(x) &= \frac{1}{2\pi}\int_0^{2\pi} (A(x-\alpha\cos\phi)^4 - B(x-\alpha\cos\phi)^2)\cos(\phi)d\phi \\
&= -\frac{1}{2}\alpha\pi^2 x(3A\alpha^2 - 2B + 4Ax^2) && (3.2)\\
V_2(x) &= \frac{1}{2\pi}\int_0^{2\pi} (A(x-\alpha\cos\phi)^4 - B(x-\alpha\cos\phi)^2)\cos(2\phi)d\phi \\
&= \frac{1}{4}\alpha^2\pi^2(-B + A(\alpha^2+6x^2)) && (3.3)\\
V_3(x) &= \frac{1}{2\pi}\int_0^{2\pi} (A(x-\alpha\cos\phi)^4 - B(x-\alpha\cos\phi)^2)\cos(3\phi)d\phi \\
&= -\frac{1}{2}A\alpha^3\pi^2 x && (3.4)\\
V_4(x) &= \frac{1}{2\pi}\int_0^{2\pi} (A(x-\alpha\cos\phi)^4 - B(x-\alpha\cos\phi)^2)\cos(4\phi)d\phi \\
&= \frac{1}{16}A\alpha^4\pi^2 && (3.5)\\
V_5(x) &= \frac{1}{2\pi}\int_0^{2\pi} (A(x-\alpha\cos\phi)^4 - B(x-\alpha\cos\phi)^2)\cos(5\phi)d\phi \\
&= 0 && (3.6)\\
\text{Similarly } V_6(x) &= V_7(x) = V_8(x)\ldots = V_n(x) = 0; n >= 5 && (3.7)
\end{aligned}
$$

As shown in [Fig.3.1], the classical variable substitution makes the potential function to be parametrically dependent on $\alpha(t)$ and therefore as α changes with time the potential as well as its corresponding wavepacket also changes adiabatically.

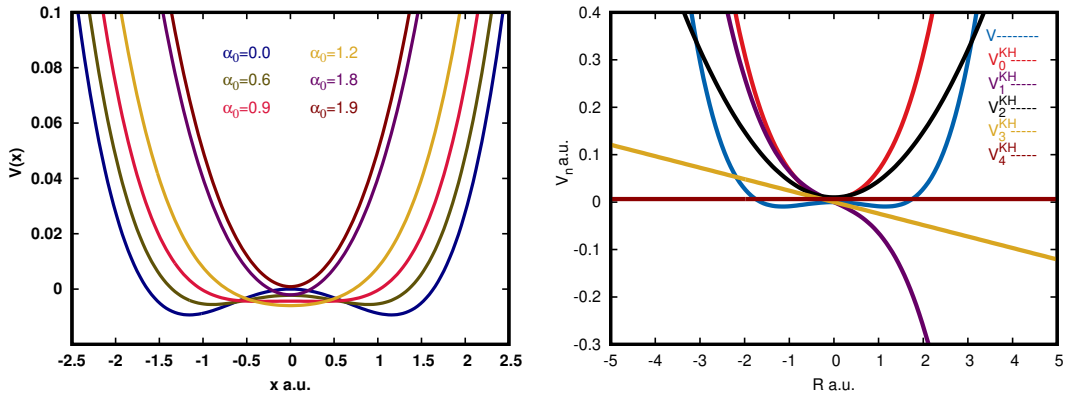

FIGURE 3.1: **(a)**Adiabatic change in symmetric double well potential as a function of $\alpha(t)$ upon KH transformation. **(b)**The KH harmonics of the double well potential at α_0=1.80. For this potential the KH harmonics above V_4^{KH} are zero.

3.1.1 Laser Form

To carry out dynamics of the wavepacket on the model potential, the oscillating electric field used is:

$$\vec{\alpha}(t) = \begin{cases} \alpha_0 \sin^2\left[\frac{\pi}{2}\frac{t}{t_{on}}\right]\cos\omega t, & 0 \le t \le t_{on} \\ \alpha_0 \cos\omega t, & t_{on} < t \end{cases} \tag{3.8}$$

where α_0 is the laser parameter defined as $\alpha_0 = \frac{\epsilon_0}{\omega^2}$, ϵ_0 is the peak field strength, ω is the field frequency and t_0 is the rise time of the laser pulse. The form of the pulse is shown in [Fig.3.2]. The frequency of the laser pulse is 2.434×10^{14} Hz (1231 nm) which is the off-resonant frequency so that the laser does not lead to excitation of the wavepacket. The peak intensity is of the order of 10^{13} W/cm^2 which is not too high to avoid the various modes of ionization. The pulse rises smoothly as the peak intensity is obtained after twenty optical cycles which gives sufficient time for the wavepacket to adjust itself to the oscillating electric field.

3.1.2 Wavepacket Dynamics using Recursive KH (t,t′)

For the chosen symmetric double well potential, there are only four eigenstates below the barrier as shown in [Fig. 3.3a]. Because of the symmetry of the double

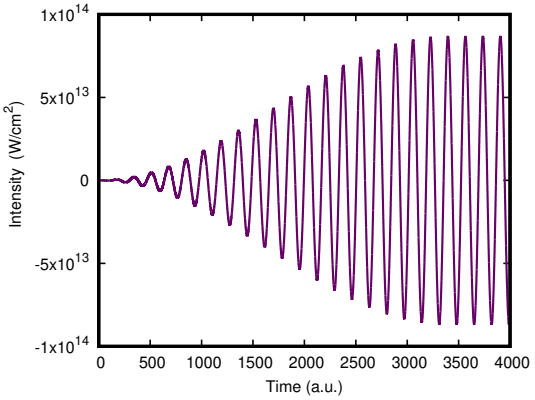

FIGURE 3.2: The oscillating electric field used to carry out wavepacket propagation in the case of symmetric double well. The peak intensity of the field is obtained after 20 optical cycles which gives sufficient time for the wavepacket to adjust itself to the oscillating electric field. The offresonant frequency (2.434×10^{14} Hz) of the pulse is chosen so that the laser does not lead to the excitation of wavepacket.

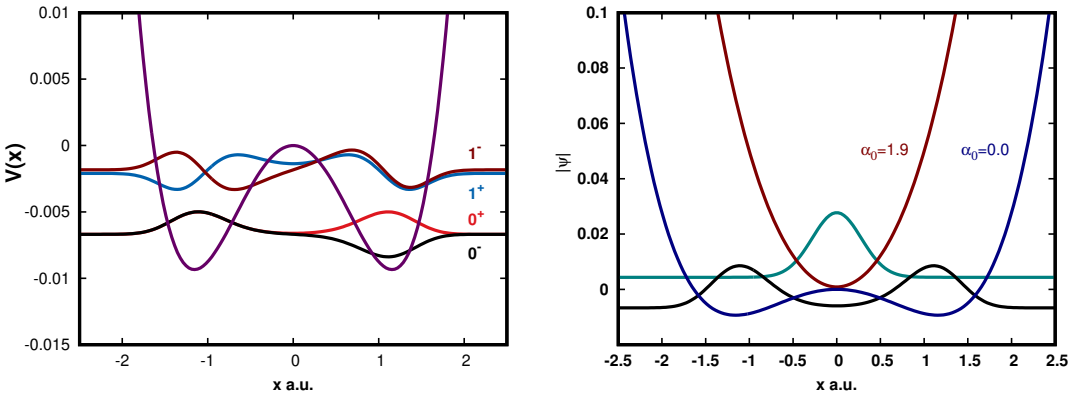

FIGURE 3.3: **(a)**Quantum tunneling in the eigenstates of the symmetric double well below the potential barrier. **(b)**The corresponding groundstate eigenvector of the double well potential for laser parameters: $\alpha_0 = 0.0$ a.u. and $\alpha_0 = 1.9$ a.u.

well, the two wells share an equal probability to hold the electron. The symmetric double well is a prototype model of quantum tunneling which implies that the electron can tunnel through the barrier and can be in either well.[1] Hence, the first two eigenstates of the system are also nearly degenerate.

Before performing the time-dependent dynamics calculation, it is essential to discuss the results of time-independent KH calculation so that the expected result from the dynamics is known. The initial wavepacket as shown in [Fig.3.3b] is

the ground state eigenvector of the Hamiltonian comprising of the kinetic energy matrix, set up using the Fourier Grid Method, [9] and the double well potential along the diagonal of the Hamiltonian matrix. The dimension of the Hamiltonian matrix on the numerical grid is (100×100). As the potential adiabatically changes from double well to single well as a function of the laser parameter $\alpha(t)$, the wavepacket also gets transformed. The time-independent KH calculations reveal that the bi-lobal wavepacket should converge and stabilize exactly at the position of the barrier of the symmetric double well. This is expected from the time-dependent wavepacket propagation in the presence of the driving laser pulse.
The propagation of the wavepacket, which is the ground state eigenvector of the symmetric double well potential, is carried out in the KH gauge in the presence of the oscillating electric field as mentioned in [section 3.1.1]. The laser pulse reaches its peak intensity after 20 optical cycles which gives a rise time of about 3400 a.u. which implies that the rise of the field is slow enough so that the wavepacket can adjust itself to the external field. The aim of the dynamics calculation is to stabilize the wavepacket on top of the potential barrier of the symmetric double well as revealed from the time-independent KH calculation. This is eventually achieved as the laser field rises and the dichotomous wavepacket evolves into the monotomic wavepacket exactly at the position of the barrier in the laboratory frame as shown in [Fig.3.4].

3.1.3 Convergence on the number of Floquet channels

The test for the convergence of the propagated wavepacket with respect to the number of Floquet channels is carried out when the laser field reaches its peak intensity. To perform the convergence calculation, wavepacket the dynamics is carried out by increasing the number of Floquet channels in each calculation. A *difference vector* is defined as the difference of wavepackets obtained as the pulse reaches its peak intensity for two consecutive dynamics calculation. The Hilbert norm of the difference vector is calculated as a measure of convergence over the Floquet channels. The Hilbert norm of a complex vector $x = \{ x_1, x_2, \ldots, x_n \}$ is

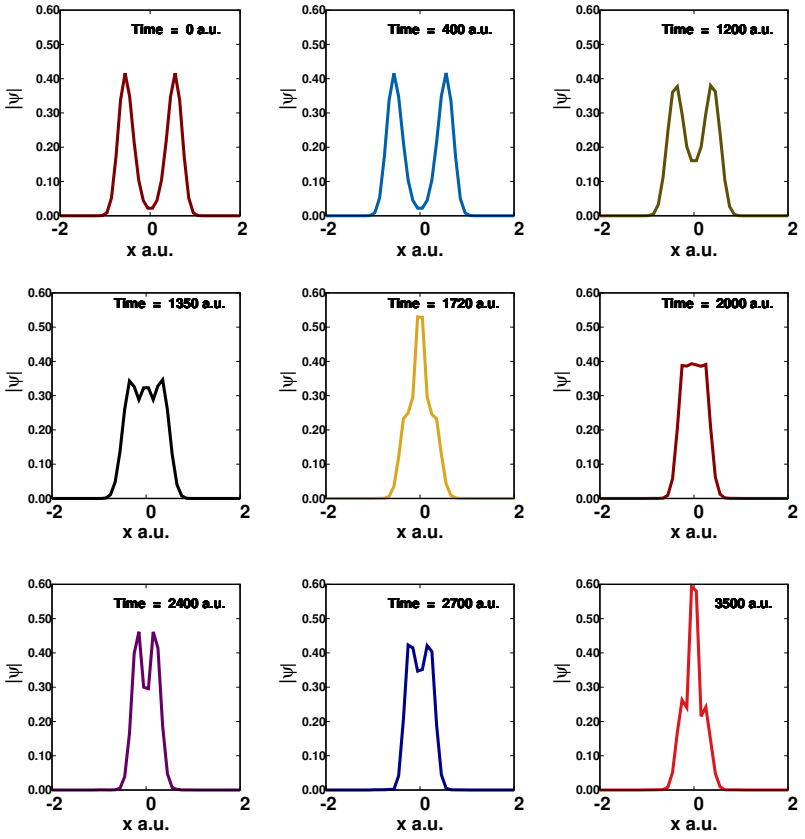

FIGURE 3.4: Time evolution of the wavepacket in presence of the oscillating electric field. The laser pulse reaches its peak intensity near 3400 a.u., i.e., the pulse is allowed to rise for 20 optical cycles. The dimension of field free Hamiltonian on the numerical grid is taken to be (100×100). As the laser intensity increases, the dichotomous wavepacket gets transformed to monotomic wavepacket at peak intensity and gets stabilized at top of the barrier of the symmetric double well potential.

defined as:

$$\|x\| = \sqrt{\sum_{k=1}^{n} x_k . x_k} \tag{3.9}$$

The Hilbert norm is tabulated alongside the number of Floquet channels in [Table 3.1]. The propagation of the wavepacket is performed in the presence of the oscillating electric field as mentioned in section 3.1.1 for time-step of 0.05 a.u. The decreasing values of the Hilbert norm with increase in the number of Floquet channels shows good convergence of the wavepacket.

TABLE 3.1: Hilbert norm of the difference vector as a measure of test for convergence over the number of Floquet channels.

N_F	Hilbert Norm
2	2.8832×10^{-2}
3	1.6664×10^{-2}
4	6.5267×10^{-3}
5	1.9323×10^{-3}
6	7.3401×10^{-4}
7	3.0985×10^{-4}
8	1.2853×10^{-4}
9	5.0726×10^{-5}
10	2.1750×10^{-5}
11	9.8341×10^{-6}
12	4.7071×10^{-6}
24	2.4918×10^{-9}

TABLE 3.2: Hilbert norm of the difference vector as a measure of test for convergence over time step.

$\triangle$t	Hilbert Norm
0.50-0.25	2.6277×10^{-2}
0.25-0.10	2.1869×10^{-2}
0.10-0.05	3.8232×10^{-3}
0.05-0.01	4.7926×10^{-4}

3.1.4 Convergence on time-step

The initial wavepacket is propagated in the presence of intense laser field till the peak intensity of field is reached. The propagation is carried out for different time-steps and the Hilbert norm of the difference wave vector, as mentioned in [section 3.1.3] is calculated as a measure of the convergence. The calculation is performed for 5 Floquet channels in the presence of the oscillating electric field. With decreasing time step, better convergence of the propagated wavepacket is obtained which is depicted by the decreasing values of the Hilbert norm of the difference vector [see Table 3.2].

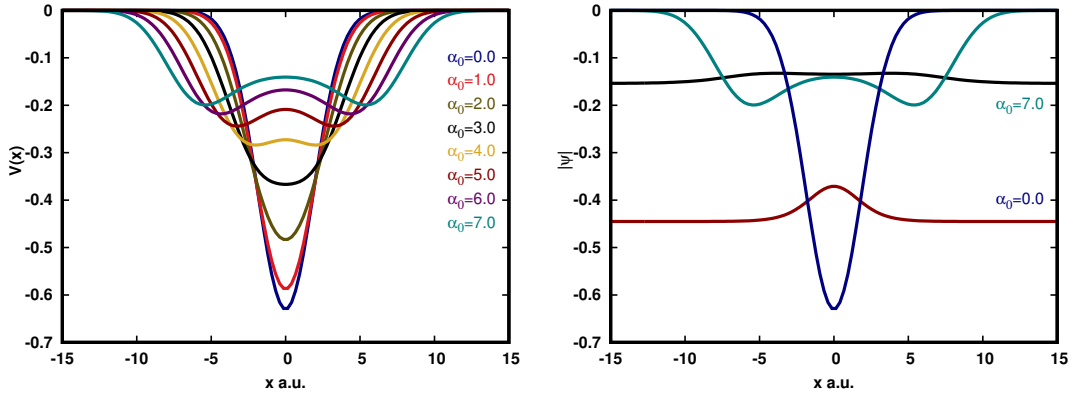

FIGURE 3.5: **(a)**Adiabatic change in the Xenon model potential as a function of $\alpha(t)$ upon the KH transformation. **(b)**The groundstate eigenvector of the potential resulting from the time-independent KH calculation for laser parameters: $\alpha_0 = 0.0$a.u. and $\alpha_0 = 7.0$ a.u. It is obtained by diagonalizing the Hamiltonian comprising of kinetic energy matrix constructed using Fourier Grid method and the time averaged potential in the diagonal.

3.2 Case 2: The Xenon Model Potential

The dynamics calculation performed for the symmetric double well potential system validates the application of the recursive algorithm in (t,t′) formalism for an oscillating electric field. Further testing is done by the application of the recursive algorithm for the Xenon model potential system where the objective is to observe the dichotomy of wavepacket in intense laser fields in the KH frame of reference. Also, to avoid the reflection of wavepacket near the edges of the finite grid, the complex absorbing potential method is employed.[10]

The functional form of the Xenon model potential is $V(x) = -0.63e^{-0.1424x^2}$ and following the KH transformation, the parametric dependence of the potential on the laser parameter i.e. $\alpha(t)$ yields a double well potential for its peak value and its corresponding eigenvector also gets splitted into a dichotomous wavepacket [see Fig. 3.5].

The harmonics of the KH potential i.e. the Fourier components of the Xenon model potential, given by $V_n(x) = \frac{1}{2\pi}\int_0^{2\pi} V(x_{KH} + \alpha_0 \cos(n\omega t))\cos(n\omega t)dt$ are not analytically calculable. So, numerical integration is performed using Gauss-Legendre integration scheme to evaluate the KH harmonics. Since, in the KH frame a classical variable substitution $x_{KH} = x - \alpha(t)e_Z$ is made which makes

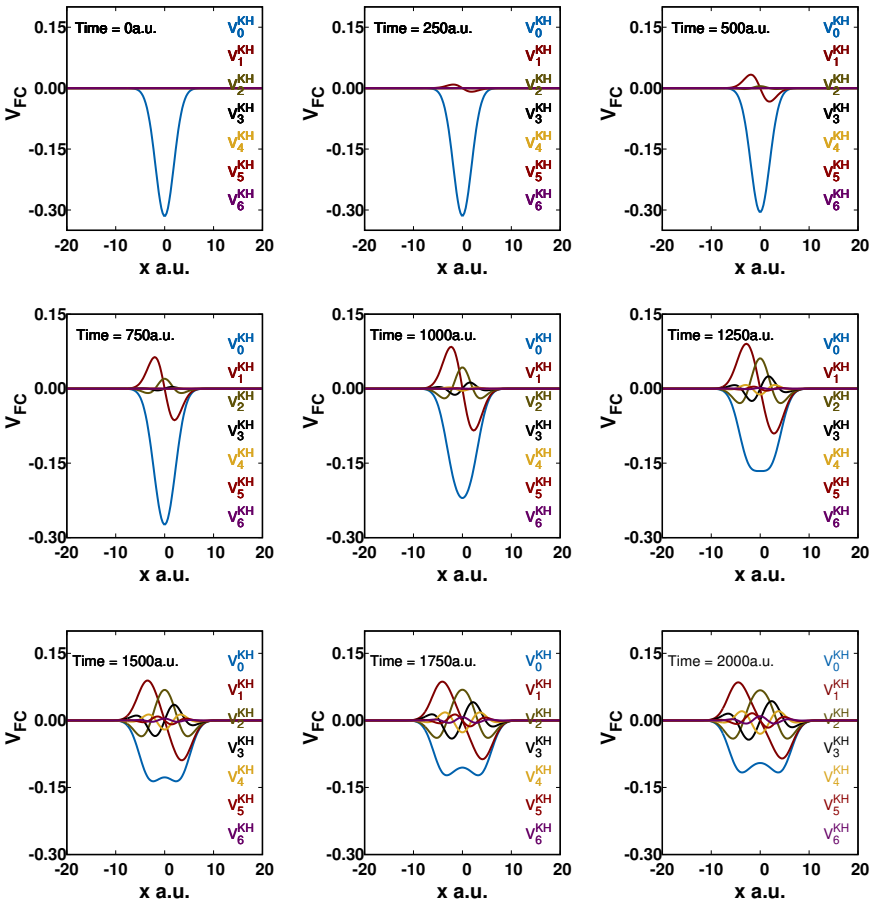

FIGURE 3.6: Time evolution of the KH harmonics of the Xenon model potential. The magnitude of the higher KH harmonics increases with time. As $V_n(x) = \frac{1}{2\pi}\int_0^{2\pi} V(x_{KH} + \alpha_0 \cos(n\omega t))\cos(n\omega t)dt$, so, apart from the zeroth harmonic all other harmonics diminishes to zero because of the rapidly oscillating $\cos(n\omega t)$ term.

the KH harmonics parametrically dependent on the laser parameter $\alpha(t)$. As the intensity of the continuous wave laser rises, the magnitude of the higher order KH harmonics inflates as shown in [Fig.3.6]. However, the zeroth order KH harmonic is still dominant over the other higher order harmonics. These higher KH harmonics, responsible for ionization, diminishes to zero because of the rapidly oscillating $\cos(n\omega t)$ term.

Not only the higher order KH harmonics diminishes to zero but also the magnitude of the higher KH harmonics is also nearly zero which is depicted in [Fig.3.7] for a fixed value of $\alpha_0 = 5.5a.u$. So, to save upon the computational cost only first nine Fourier components are included in the dynamics calculation.

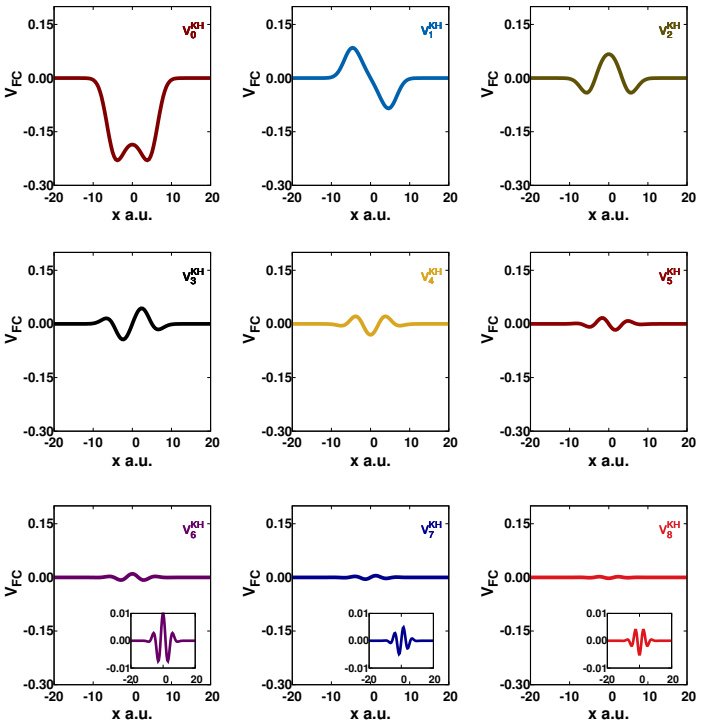

FIGURE 3.7: The Fourier components of Xenon model potential for a fixed value of $\alpha_0 = 5.5a.u.$ The magnitude of the higher KH harmonics is nearly zero and so can be avoided in the computational calculation while contructing the Floquet Hamiltonian.

3.3 Complex Absorbing Potential (CAP)

To study the dynamics of wavepacket in a time-dependent field, a CAP was first introduced in 1986 by Kosloff and Kosloff. [11] Because of the finite size of the numerical grid, artificial reflection of the wavepacket takes place near the edges and as a result the quality of the computed results is hampered. Application of a CAP results in suppression of the reflection by absorbing the asymptotic part of the outgoing wavepacket. [10] Therefore, in the time-dependent picture, the CAP serves to save upon the computational cost by avoiding the use of large grids.

To address the problem at hand, a quadratic CAP of the form, V_{cap} = -0.01i|x-$x_0|^2$, is used beyond the classical turning points of the oscillating xenon model potential as shown in [Fig.3.8] in the presence of laser field. In the KH frame, the CAP is employed only at the zeroth block for computational feasibility. The CAP is not used for other blocks because for the analytical block-diagonalization

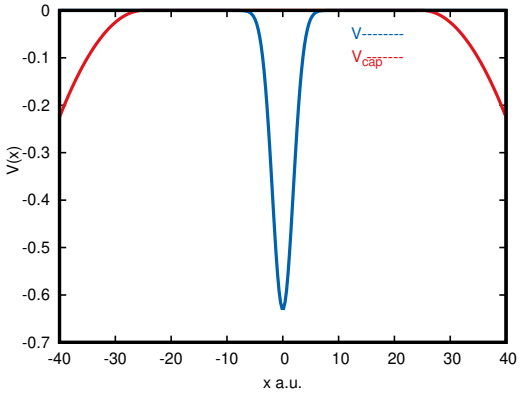

FIGURE 3.8: The imaginary part of the complex absorbing potential is plotted outside the classical turning point of the xenon model potential in laser. The functional form of the CAP is quadratic $V_{cap} = -\lambda|x - x_0|^2$ in the imaginary plane. λ is the CAP strength parameter which is 0.01 in this case.

of the exponential of the KH harmonic matrices the eigenvalues of representative matrices, given in Appendix 1, are used. These eigenvalues are both positive and negative. Now, because the CAP employed is a negative quadratic so, its multiplication with negative eigenvalues gives a positive value whose exponential diverges. And hence, the CAP is only applied at the zeroth block only.

3.4 Wavepacket Dynamics using Recursive KH (t,t′)

In quantum mechanics the points at which the potential energy of the system equals the total energy are referred as classical turning points. In the accelerated frame of reference, the application of high intensity laser field results in periodic oscillations of the potential. The dynamics of the wavepacket is carried out in the presence of oscillating laser field as mentioned in section 3.1.1 with peak intensity of the order of 10^{15} W/cm^2 and frequency of 6.58×10^{14} Hz (455.6 nm). At peak intensity, the objective of the dynamics calculation is to stabilize the initial wavepacket at the classical turning points of laser interacted xenon model potential system.

From [Fig.3.9], the dynamics calculation reveals the splitting of wavepacket in

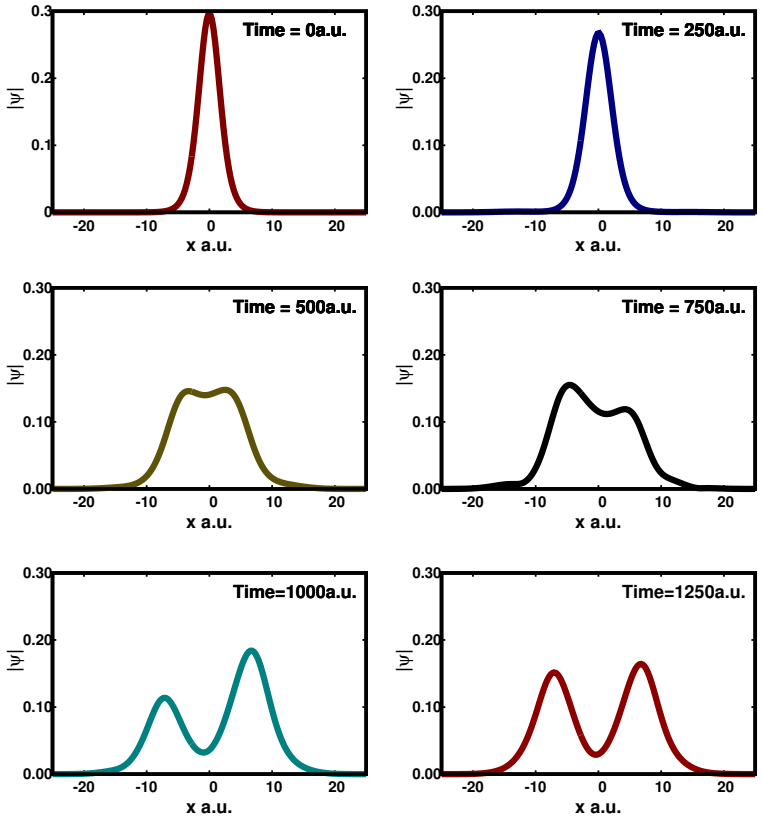

FIGURE 3.9: Time evolution of the wavepacket in the presence of oscillating electric field. As the intensity of the laser field rises, the wavepacket gets splitted into a dichotomous wavepacket with the two lobes stabilized at the classical turning points of the xenon model potential in the length gauge in the presence of laser.

the intense laser field and as the field reaches its peak intensity, there is no further splitting of the wavepacket, with the dichotomous lobes stabilizing at the exact positions of the classical turning points of the xenon model potential system in the length gauge in the laser field. From the time-independent KH calculation [see Fig. 3.5], it was expected that the initial wavepacket gets splitted into a dichotomous wavepacket with the localization of the two lobes over the two wells of the transformed KH potential. This is confirmed and validated from the dynamics calculation as well.

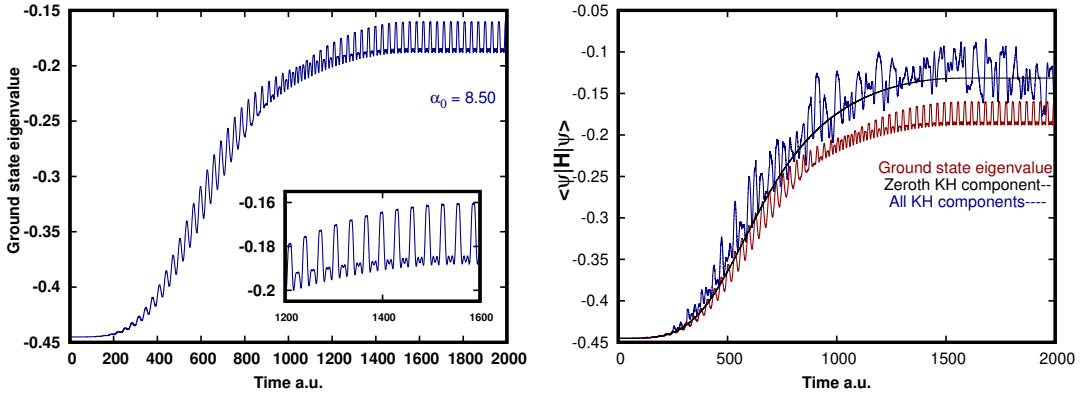

FIGURE 3.10: **(a)**The time-dependent Hamiltonian is diagonalized at each time step to obtain the plot of ground state eigenvalue as a function of $\alpha(t)$. An analogous dichotomy is obtained at peak intensity similar to the dichotomy of wavepacket. **(b)**A comparison is made between the expectation values of wavepacket corresponding to the Hamiltonian comprising of all KH components to that of Hamiltonian comprising of just the zeroth KH harmonic. The former expectation value curve oscillates through the latter which implies that the dynamics is mostly driven by the zeroth KH harmonic.

3.5 Energy Expectation value of the propagated wavepacket

As the initial wavepacket is evolved in the presence of intense laser field, the ground state eigenvalue of the time-dependent Hamiltonian is evaluated at each time step till stabilization is achieved. As the field interacts with the potential system, the eigenvalue increases in an oscillatory manner. The dynamics calculation revealed that the dichotomy of wavepacket starts around time=1000 a.u. In a similar manner, amidst the oscillatory incrementation of the eigenvalue with time, it is observed that an analogous dichotomy in the eigenvalue value plot starts around time=1000 a.u. [see Fig.3.10].

The expectation value of the propagated wavepacket is plotted in [Fig. 3.11b]. A comparison is made between the expectation values of the wavepacket for the Hamiltonian consisting of all the KH components and for the Hamiltonian consisting only of the zeroth Fourier component. The expectation values of the wavepacket corresponding to the former Hamiltonian oscillates through the other curve which validates the fact that the dynamics is mostly driven by the zeroth

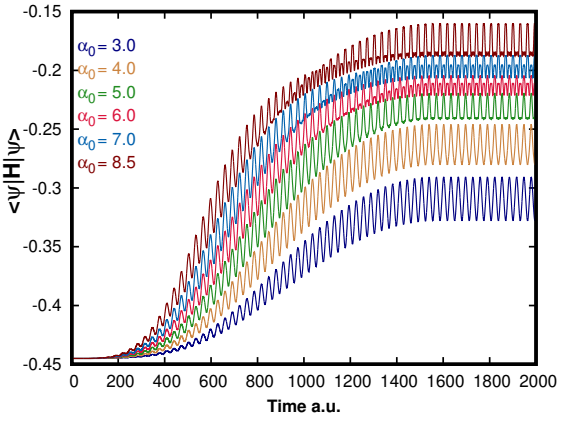

FIGURE 3.11: The ground state eigenvalue of the time-dependent Hamiltonian is plotted for various values of α_0. Just as the dichotomy in wavepacket appears only above a certain threshold value of α_0, similarly the dichotomy in the eigenvalue curve appears only above the same α_0.

KH harmonic. Also, the expectation value of the wavepacket is nearly equal to the ground state eigenvalue which signifies that the dynamics calculation is clean.

To consolidate the point about the dichotomy arising in the ground state eigenvalue of the time-dependent Hamiltonian with rise in the intensity of laser, the calculation is run for various values of α_0. The results reveal that just as the splitting of the wavepacket takes place only after a threshold value of α_0, a similar splitting is obtained in the eigenvalue value plot only after α_0 value is incremented after a certain threshold. As can be seen in [Fig.3.10], that threshold α_0 is 6.0 a.u. when the dichotomy starts appearing.

Therefore, the recursive algorithm in (t,t′) for quantum dynamics in the Kramers-Henneberger frame of reference is implemented for any number of Floquet channels and KH harmonics. The test calculations on symmetric double well and xenon model potential validates the proposed recursive algorithm for time-propagation in the KH gauge.

3.6 Future Work

We are interested in the extension of the developed (t,t′) recursive algorithm. Some of the plans for future work are:

1. A recursive implementation of (t,t′,t″) method for time propagation in the presence of a Gaussian pulse.

2. Carry out quantum dynamics of wavepacket for a real atomic system.

References

[1] F. Großmann, T. Dittrich, P. Jung and P. Hänggi, *Phys. Rev. Lett.* **67**, 516 (1991).

[2] F. Großmann and P. Hänggi, *Europhys. Lett.* **18**, 571 (1992).

[3] F. Großmann, P. Jung, T. Dittrich and P. Hänggi, *Z. Phys. B: Condens. Matter* **84**, 315 (1991).

[4] M. Grifoni and Hänggi, *Phys. Rep.* **304**, 229 (1998).

[5] P. Löwdin, *Rev. Mod. Phys.* **35**, 724 (1963).

[6] G. Campoy, A. Palma and L. Sandoval, *Int. J. Quant. Chem.* Quantum Chemistry Symposium **23**, 355 (1989).

[7] R. L. Samorjai, D. F. Horning *J. Phys. Chem.* **36**, 1980 (1962).

[8] Wolfram Research, Inc., *Mathematica*, Version 11.3, Champaign, IL, (2018)

[9] David J. Tannor, *Introduction to Quantum Mechanics: A Time-Dependent Perspective.* Sausalito, Calif: University Science Books (2007).

[10] U. V. Riss and H. -D. Meyer, *J. Phys. B: At. Mol. Opt. Phys.* **26**, 4503 (1993).

[11] R. Kosloff and D. Kosloff, *J. Comput. Phys.* **63**, 362 (1986).

Appendix A

Analytical Block Diagonalization

The propagator for time propagation is evaluated by using the split in which the exponential of the block matrices needs to be computed. The first step to compute the exponential is to block-diagonalize the KH harmonic matrices. The KH harmonic matrices can be constructed for any number of Floquet channels. For 2 Floquet channels and 5 KH harmonics, the off-diagonal block matrices which need to be diagonalize are:

$$\begin{bmatrix} 0 & [V_1^{KH}] & 0 & 0 & 0 \\ [V_1^{KH}] & 0 & [V_1^{KH}] & 0 & 0 \\ 0 & [V_1^{KH}] & 0 & [V_1^{KH}] & 0 \\ 0 & 0 & [V_1^{KH}] & 0 & [V_1^{KH}] \\ 0 & 0 & 0 & [V_1^{KH}] & 0 \end{bmatrix} \quad \begin{bmatrix} 0 & 0 & [V_2^{KH}] & 0 & 0 \\ 0 & 0 & 0 & [V_2^{KH}] & 0 \\ [V_2^{KH}] & 0 & 0 & 0 & [V_2^{KH}] \\ 0 & [V_2^{KH}] & 0 & 0 & 0 \\ 0 & 0 & [V_2^{KH}] & 0 & 0 \end{bmatrix}$$

$$\begin{bmatrix} 0 & 0 & 0[V_3^{KH}] & 0 \\ 0 & 0 & 0 & 0 & [V_3^{KH}] \\ 0 & 0 & 0 & 0 & 0 \\ [V_3^{KH}] & 0 & 0 & 0 & 0 \\ 0 & [V_3^{KH}]0 & 0 & 0 & 0 \end{bmatrix} \quad \begin{bmatrix} 0 & 000[V_4^{KH}] \\ 0 & 000 & 0 \\ 0 & 000 & 0 \\ 0 & 000 & 0 \\ [V_4^{KH}]000 & 0 \end{bmatrix}$$

The dimensions of all these matrices are $((2 * N_f + 1) * n_x \times (2 * N_f + 1) * n_x)$, where N_f is the number of Floquet channels and n_x is the grid size. Since the complexity of diagonalization amounts to $\mathcal{O}(\mathrm{N}^3)$. So numerical diagonalization of these matrices is computationally very expensive. Hence, analytical block-diagonalization

is carried out by using the eigenvalues and eigenvectors of the following symmetric matrices:

$$\begin{bmatrix} 01000 \\ 10100 \\ 01010 \\ 00101 \\ 00010 \end{bmatrix} \quad \begin{bmatrix} 00100 \\ 00010 \\ 10001 \\ 01000 \\ 00100 \end{bmatrix} \quad \begin{bmatrix} 00010 \\ 00001 \\ 00000 \\ 10000 \\ 01000 \end{bmatrix} \quad \begin{bmatrix} 00001 \\ 00000 \\ 00000 \\ 00000 \\ 10000 \end{bmatrix}$$

For N_f number of Floquet channels, the dimension of the above symmetric matrices is $((2 * N_f + 1) \times (2 * N_f + 1))$. The analytical block-diagonalization of the first KH harmonic matrix is shown as a prototype. Let $\mathrm{a}_i^1 (i = 1, 2, 3, 4, 5)$ be the eigenvalues and U_1 contains the eigenvectors of the matrix whose elements are $\delta_{n,n'\pm1}$. Then, the block-diagonalization of the V_1^{KH} is given by:

$$V_1^d = \begin{bmatrix} [V_1^{KH} * a_1^1] & 0 & 0 & 0 & 0 \\ 0 & [V_1^{KH} * a_2^1] & 0 & 0 & 0 \\ 0 & 0 & [V_1^{KH} * a_3^1] & 0 & 0 \\ 0 & 0 & 0 & [V_1^{KH} * a_4^1] & 0 \\ 0 & 0 & 0 & 0 & [V_1^{KH} * a_5^1] \end{bmatrix}_{[(2N_f+1)*n_x,(2N_f+1)*n_x]}$$

In the diagonal form, the exponential of a matrix is just the exponential of its eigenvalues. And, $V_1^{KH} = U_1 V_1^d U_1^\dagger$. Likewise, all the KH harmonic matrices are analytically block-diagonalize and hence, the propagator is evaluated.

There is still a need to compute the eigenvalues and eigenvectors of the representative symmetric matrices. For $\delta_{n,n'\pm1}$ matrix, the analytical expression for the eigenvalues is $\cos(\frac{k\pi}{N_f+1})$ (k=1,2,...,2*N_f+1).[1] And, the unitary matrix form of stacked up eigenvectors is:

$$U_{ij} = \sqrt{\frac{2}{N_f + 1}} \sin(i\tau_j) \tag{A.1}$$

where $\tau_j = \frac{j\pi}{N_f+1}$ (j=1,2,...,2*N_f+1). However, for rest of the symmetric matrices the analytical expression for the eigenvalues and eigenvectors still needs to be derived. If the analytical expression is derived, there won't be any need to numerically compute and store the eigenvalues and eigenvectors. [Fig. A.1] shows a plot for the eigenvalues of the symmetric matrices on varying the number of Floquet

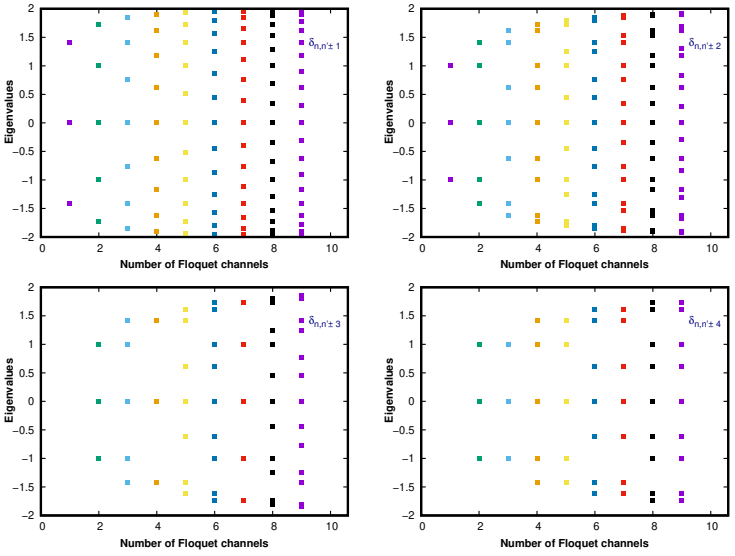

FIGURE A.1: Eigenvalues of the symmetric matrices on varying the number of Floquet channels. The elements of the symmetric matrices are given by $\delta_{n,n'\pm n}$. The analytical expression for the eigenvalues of the matrix with $\delta_{n,n'\pm 1}$ is known. For the other matrices, the expression still needs to be derived.

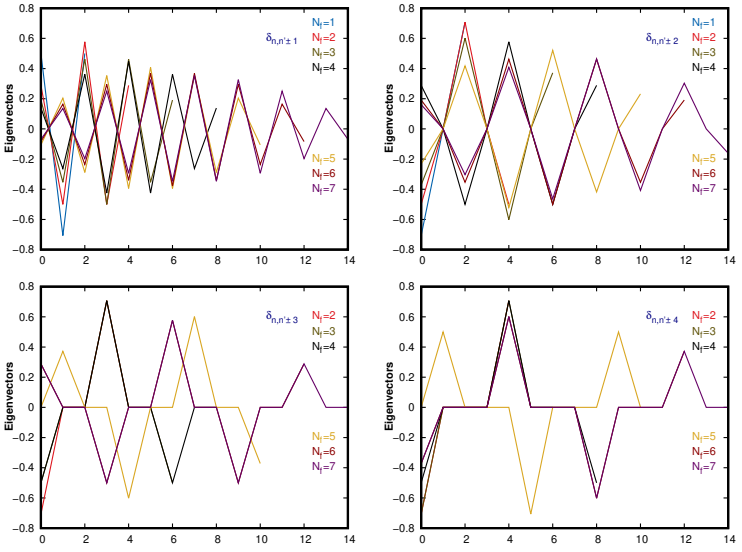

FIGURE A.2: The first eigenvector of the symmetric matrices on varying the number of Floquet channels. Similar to [Fig. A.1], the analytical expression for the eigenvectors of the matrix with $\delta_{n,n'\pm 1}$ is known. For the other matrices, the expression still needs to be derived.

channels. For $\delta_{n,n'\pm 1}$, the analytical expression for the eigenvectors is given in Eq. [A.1]. The plot of first eigenvector for each unitary matrix is given in [Fig. A.2] and its analytical expression is still a problem to address.

References

[1] S. Chu, *J. Chem. Phys.* **75**, 2215 (1981).

Appendix B

Codes

The following code is written in **Fortran90** [1] programming language to carry out time propagation of the test cases described in Chapter 3. The test system taken up in this code is the symmetric double well potential system.

B.1 Packages Used

LAPACK [2] (Linear Algebra PACKage): Used for diagonalization of the matrices.

B.2 Compilers Used

gfortran (the GNU Fortran compiler)

B.3 Compilation Instruction

Use the following command on terminal: gfortran codefile.f90 -llapack -lblas
codefile.f90 is the only input file consisting of the subroutines: *recur1*, *recur2* and *DSYEV_WT_EIGVECS*

B.4 Code

```
!Code to perform time propagation of wavepacket for symmetric double well po-
tential system.
!Author :: Rishabh Gupta
!Date   :: 15/1/2019
      program ttprime_ method
      implicit none
!*****************Variables declaration**********************!
      integer ( kind = 4 ), parameter :: num = 100
      real ( kind = 8 ), parameter :: pi = acos(-1.0d0)
      complex ( kind = 8 ), parameter :: ci = (0.0d0,1.0d0)
      integer ( kind = 4 ) :: i, i1, j, j1, c, c1, k
      real ( kind = 8 ) :: A, B, x, xmax, xmin, dx, m, n, dk
      complex ( kind = 8 ) :: s, z, w
      real ( kind = 8 ), allocatable :: T(:,:), H0(:,:), H1(:,:)
      real ( kind = 8 ), allocatable :: V(:,:), V_U(:,:), V_J(:,:), V_eval(:,:)
      real ( kind = 8 ), allocatable :: eval(:), eigvals(:), evecs(:,:), eigvecs(:,:)
      real ( kind = 8 ), allocatable :: psi(:,:)
      complex ( kind = 8 ), allocatable :: H0_exp(:,:), H0_U(:,:), H0_sm(:,:)
      complex ( kind = 8 ), allocatable :: U(:,:), UT(:,:), pro(:,:), H0_UUT(:,:)
!*****************Floquet variables**************************!
      integer ( kind = 8 ), parameter :: Nf = 6
      integer ( kind = 8 ) :: fch, fld
      real ( kind = 8 ) :: omega, alpha, a0, n
      complex ( kind = 8 ), allocatable :: evec_fl(:)
      complex ( kind = 8 ), allocatable :: M_nw(:), P_fl(:), PU(:)
!*****************Time variables*****************************!
      integer ( kind = 4 ), parameter :: tsteps = 30000
      integer ( kind = 4 ) :: t1
      real ( kind = 8 ) :: dt, time, ton
!*****************Constants**********************************!
      A = 0.005224862d0 ; B = 0.0139753572d0
```

```
      a0 = 1.80d0 ; omega = 0.037d0
      ton = 20.0d0*(2.0d0*pi/omega)
      fch = 2*Nf+1 ; fld = fch*num
      xmax = 10.0d0 ; xmin = -10.0d0
      dx = (xmax-xmin)/float(num-1)
      dk = 2.0d0*pi/(num*dx)
      dt = 0.1d0
      w = exp((2.0d0*pi*ci)/num)
      m = 1822.888d0
!*****************Matrix allocation*************************!
      allocate( T(num,num), H0(num,num), H1(num,num) )
      allocate( V(num,fch), V_U(fch*(fch-1),fch*(fch-1)) )
      allocate( V_J(fch,fch), eigvals(fch), eigvecs(fch,fch) )
      allocate( V_eval((fch-1)*fch) )
      allocate( eval(num), evecs(num,num) )
      allocate( U(num,num), UT(num,num) )
      allocate( H0_exp(fld,fld), pro(num,num) )
      allocate( evec_fl(fld), psi(fld,tsteps) )
      allocate( M_nw(fld), PU(fld) )
      allocate( H0_sm(num,num), H0_U(num,num), H0_uut(num,num) )
      allocate( P_fl(fld), P_uut(fld) )
!*****************Fourier grid Hamiltonian*******************!
      T = 0.0d0
      do k = 0, num/2
         T(k+1,k+1) = (0.5d0/m)*(k*dk)**2
      enddo
      c = (num/2)+2
      do k = -(num/2)+1,-1
         T(c,c) = (0.5d0/m)*(k*dk)**2
         c = c + 1
      enddo
      U = (0.0d0,0.0d0) ; UT = (0.0d0,0.0d0)
      do i = 0, num-1
```

```
      do j = 0, num-1
        U(i+1,j+1) = w**(i*j)
        UT(i+1,j+1) = w**(-i*j)
      enddo
    enddo
    H0 = 0.0d0 ; H1 = 0.0d0
    pro = (0.0d0,0.0d0)
    pro = matmul(T,UT)
    H0 = (1.0d0/num)*matmul(U,pro)
    H1 = H0
    deallocate( T,pro,U,UT )
!******************Initial wavepacket************************!
    do i = 1, num
      x = xmax - (i-1)*dx
      H0(i,i) = H0(i,i) + A*x**4 - B*x**2
    enddo
    call DSYEV_WT_EIGVECS(H0,num,eval,evecs)
    evec_fl = 0.0d0 ; c1 = 0
    do j1 = -Nf , Nf
      do i1 = 1,num
        evec_fl(c1*num+i1) = evecs(i1,1)
      enddo
    c1 = c1 + 1
    enddo
!******************Exponential of number matrix***************!
    M_nw = 0.0d0 ; n = -Nf*1.0d0
    do j = 1, fch
      do i = 1, num
        M_nw((j-1)*num+1) = exp(-0.50d0*ci*n*omega*dt)
      enddo
    n = n + 1.0d0
    enddo
!**********Unitary matrices for analytical diagonalization*******!
```

```
      V_U = 0.0d0 ; V_eval = 0.0D0
      do j = 1, fch-1
       V_J = 0.0d0
       do i = 1, fch-j
          V_J(i,i+j) = 1.0d0
         V_J(i+j,i) = 1.0d0
       enddo
       eigvals = 0.0d0
       eigvecs = 0.0d0
       call DSYEV_WT_EIGVECS(V_J,fch,eigvals,eigvecs)
       do i = 1, fch
       do k = 1, fch
          V_U((j-1)*fch+i,(j-1)*fch+k) = eigvecs(i,k)
       enddo
       V_eval((j-1)*fch+i) = eigvals(i)
       enddo
      enddo
!**************Time Propagation starts*****************************!
      do t1 = 1, tsteps
       time = (t1-1)*dt
       if (time < ton) then
        alpha = a0*(sin(pi*time/(2*ton))**2)
       else
        alpha = a0
       endif
       !****KH harmonics construction****!
       V = 0.0d0 ; H0 = 0.0d0
       do i = 1,num
        x=xmax-(i-1)*dx
        V(i,1) = A*( x**4 + 3.0d0*(alpha**2)*x**2 + &
             (3.0d0/8.0d0)*alpha**4 ) - B*(x**2 + 0.5d0*alpha**2)
        V(i,2) = -0.5d0*0.5D0*alpha*x*( 3.0d0*A*alpha**2 - &
             2.0d0*B + 4.0d0*A*x**2 )
```

```
  V(i,3) = 0.5d0*0.25d0*(alpha**2)*( -B + A*(alpha**2 + 6.0d0*x**2) )
  V(i,4) = -0.5d0*0.50d0*A*(alpha**3)*x
  H0(i,i) = H0(i,i) + V(i,1)
enddo
V(:,5) = 0.5d0*(1.0d0/16.0d0)*A*alpha**4
!***********************!
P_fl = (0.0d0,0.0d0)
P_fl(:) = M_nw(:) * evec_fl(:)
!****Recursive subroutine-1****!
CALL recur1( P_fl, fch-1, fch, fch, fld, num, V_U, V_eval, V, dt)
!************************!
H0_exp = (0.0d0,0.0d0)
eval = 0.0d0 ; evecs = 0.0d0
call DSYEV_WT_EIGVECS(H0,num,eval,evecs)
do i = 1, num
   H0_sm(i,i) = exp(-ci*dt*eval(i))
enddo
H0_U = matmul(evecs,H0_sm)
H0_uut = matmul(H0_U,transpose(evecs))
P_uut = (0.0d0, 0.0d0)
do i = 1, fch
  do j = 1, num
  s = (0.0d0, 0.0d0)
  do k = 1, num
    s = s + (H0_uut(j,k)*P_fl((i-1)*num+k))
  enddo
  P_uut((i-1)*num+j) = s
  enddo
enddo
P_uut = (0.0d0,0.0d0)
do i = 1, fld
  s = (0.0d0,0.0d0)
  do j = 1, fld
```

```
        s = s + H0_exp(i,j) * P_fl(j)
       enddo
       P_uut(i) = s
      enddo
      P_fl = (0.0d0,0.0d0)
      P_fl = P_uut
      !****Recursive subroutine-2******!
      CALL recur2( P_fl, 1, fch, fch, fld, num, V_U, V_eval, V, dt )
      !*********************************!
      evec_fl = (0.0d0,0.0d0)
      evec_fl(:) = M_nw(:) * P_nw(:)
      psi(:,t1) = abs(evec_fl(:))
      c2 = 0
      do j1 = -Nf,Nf
       do i1 = 1,num
       evec_fl(c2*num+i1) = exp(ci*j1*omega*time)*evec_fl(c2*num+i1)
       enddo
      c2 = c2 + 1
      enddo
     enddo
!************Time Propagation Ends**********************!
     open(10,file="tprop.dat")
     do i = Nf*num+1,(Nf+1)*num
       write(10,*)(psi(i,j),j=1,tsteps)
     enddo
     deallocate( H0,H1,eval,evecs )
     deallocate( evec_fl,psi, P_uut, H0_exp )
     deallocate( M_nw, P_fl, V_U, V_eval )
     end
!*****************************************************!
     recursive subroutine recur1 ( P_fl, N, fch, fch, fld, num, V_U, V_eval, V, dt )
     implicit none
     integer ( kind = 4 ) :: N, num, fch, fld
```

```
      complex ( kind = 8 ), parameter :: ci = (0.0d0,1.0d0)
      complex ( kind = 8 ) :: s
      integer ( kind = 8 ) :: i, j, k
      real ( kind = 8 ) :: dt        real ( kind = 8 ), allocatable :: U_j(:,:), U_jt(:,:)
      complex( kind = 8 ), allocatable :: PU(:), PU2(:), PV(:), V_exp(:,:)
      complex ( kind = 8 ) :: P_fl(fld)
      real ( kind = 8 ) :: V_eval((fch-1)*fch), V(num,fch)
      real ( kind = 8 ) :: V_U(fch*(fch-1),fch*(fch-1))
     !************************!
      allocate( U_j(fch,fch), U_jt(fch,fch) )
      allocate( V_exp(fld,fld), PU(fld), PU2(fld), PV(fld) )
!*******Unitary matrix construction************!
      U_j = 0.0d0 ; U_jt = 0.0d0
      do i = 1, fch
       do j = 1, fch
        U_j(i,j) = V_U((N-1)*fch+i,(N-1)*fch+j)
       enddo
      enddo
      U_jt = transpose(U_j)
!*********************************!
      PU = (0.0d0,0.0d0)
      do j = 1, fch
       do i = 1, num
        s = (0.0d0,0.0d0)
        do k = 1, fch
         s = s + ( U_jt(j,k) * P_fl((k-1)*num+i) )
        enddo
        PU((j-1)*num+i) = s
       enddo
      enddo
      V_exp = (0.0d0,0.0d0)
      do i = 1, fch
       do j = 1, num
```

```
          V_exp((i-1)*num+j,(i-1)*num+j) = exp(-0.5d0*ci*dt* &
              ( V(j,N+1)*V_eval((N-1)*fch+i)) )
         enddo
        enddo
        PV = (0.0d0,0.0d0)
        do i = 1, fld
         PV(i) = V_exp(i,i) * PU(i)
        enddo
        PU2 = (0.0d0,0.0d0)
        do j = 1, fch
         do i = 1, num
          s = (0.0d0,0.0d0)
          do k = 1, fch
           s = s + ( U_j(j,k) * PV((k-1)*num+i) )
          enddo
          PU2((j-1)*num+i) = s
         enddo
        enddo
        P_fl = PU2
!*******call recur1 until N≥2************!
        if ( N ≥ 2) then
          call recur1( P_fl, N-1, fch, fch, fld, num, V_U, V_eval, V, dt )
       endif
        end subroutine
!*******************************************!
        recursive subroutine recur2( P_fl, N, fch, fch, fld, num, V_U, V_eval, V, dt )
        implicit none
        integer ( kind = 4 ) :: N, num, fch, fld
        complex ( kind = 8 ), parameter :: ci = (0.0d0,1.0d0)
        complex ( kind = 8 ) :: s
        integer ( kind = 8 ) :: i, j, k
        real ( kind = 8 ) :: dt          real ( kind = 8 ), allocatable :: U_j(:,:), U_jt(:,:)
        complex( kind = 8 ), allocatable :: PU(:), PU2(:), PV(:), V_exp(:,:)
```

```
      complex ( kind = 8 ) :: P_fl(fld)
      real ( kind = 8 ) :: V_eval((fch-1)*fch), V(num,fch)
      real ( kind = 8 ) :: V_U(fch*(fch-1),fch*(fch-1))
     !************************!
      allocate( U_j(fch,fch), U_jt(fch,fch) )
      allocate( V_exp(fld,fld), PU(fld), PU2(fld), PV(fld) )
!*******Unitary matrix construction************!
      U_j = 0.0d0 ; U_jt = 0.0d0
      do i = 1, fch
       do j = 1, fch
        U_j(i,j) = V_U((N-1)*fch+i,(N-1)*fch+j)
       enddo
      enddo
      U_jt = transpose(U_j)
!***********************************!
      PU = (0.0d0,0.0d0)
      do j = 1, fch
       do i = 1, num
        s = (0.0d0,0.0d0)
        do k = 1, fch
         s = s + ( U_jt(j,k) * P_fl((k-1)*num+i) )
        enddo
        PU((j-1)*num+i) = s
       enddo
      enddo
      V_exp = (0.0d0,0.0d0)
      do i = 1, fch
       do j = 1, num
        V_exp((i-1)*num+j,(i-1)*num+j) = exp(-0.5d0*ci*dt* &
            ( V(j,N+1)*V_eval((N-1)*fch+i)) )
       enddo
      enddo
      PV = (0.0d0,0.0d0)
```

```
      do i = 1, fld
       PV(i) = V_exp(i,i) * PU(i)
      enddo
      PU2 = (0.0d0,0.0d0)
      do j = 1, fch
       do i = 1, num
        s = (0.0d0,0.0d0)
        do k = 1, fch
         s = s + ( U_j(j,k) * PV((k-1)*num+i) )
        enddo
        PU2((j-1)*num+i) = s
       enddo
      enddo
      P_fl = PU2
!*******call recur2 until N≤fch-2***********!
      if ( N ≤ fch-2) then
        call recur2( P_fl, N+1, fch, fch, fld, num, V_U, V_eval, V, dt )
     endif
      end subroutine
!*****************************************!
      subroutine DSYEV_WT_EIGVECS( H, ndim, eigvals, eigvecs )
      implicit none
      integer ( kind = 4 ) :: ndim
      real ( kind = 8 ) :: H(ndim,ndim), eigvals(ndim), eigvecs(ndim,ndim)
      character ( len = 1 ), parameter :: JOBZ="V"
      character ( len = 1 ), parameter :: UPLO="L"
      integer ( kind = 4 ) :: LDA, LDWORK, INFO
      real ( kind = 8 ), allocatable :: WORK(:)
      LDA = ndim
      LDWORK = 3*ndim-1
      allocate( WORK(LDWORK) )
      call DSYEV( JOBZ, UPLO, ndim, H, LDA, eigvals, WORK, LDWORK, INFO )
      deallocate( WORK )
```

```
      eigvecs = H
      end subroutine
!*********************************************************************!
```

B.5 Sample Input File

The input file comprises of the main code with the recursive subroutines and the subroutine for the diagonalization of a matrix through LAPACK. A sample of the code file is given below:

```
      program ttprime_method
      implicit none
!*****************Variables declaration************************!
      integer ( kind = 4 ), parameter :: num = 100
      real ( kind = 8 ), parameter :: pi = acos(-1.0d0)
      complex ( kind = 8 ), parameter :: ci = (0.0d0,1.0d0)
      integer ( kind = 4 ) :: i, i1, j, j1, c, c1, k
      real ( kind = 8 ), allocatable :: T(:,:), H0(:,:), H1(:,:)
      ...
      ...
!***************Time Propagation starts*****************************!
      do t1 = 1, tsteps
       time = (t1-1)*dt
       if (time < ton) then
        alpha = a0*(sin(pi*time/(2*ton))**2)
       else
        alpha = a0
       endif
      ...
      ...
!*******call recur2 until N≤fch-2************!
      if ( N ≤ fch-2) then
         call recur2( P_fl, N+1, fch, fch, fld, num, V_U, V_eval, V, dt )
      endif
      end subroutine
```

B.6 Sample Output File

The output file consists of the absolute value of the propagated wavepacket at each time step. A sample output file is given below:

4.9109028781043885E-013	4.9107163327034147E-013	4.9115365068186922E-013
4.9118780077010322E-013	4.9087521029809780E-013	4.9023301804270620E-013
4.9299528864298955E-013	4.8791034754664045E-013	4.9428754267612438E-013
4.8852203424381249E-013	4.9368382703051147E-013	4.8831621823662732E-013
4.9383539572111971E-013	4.8805069801907139E-013	4.9392138769267964E-013
4.8832754796886164E-013	4.9391408775914684E-013	4.8826026495041950E-013
4.9411551257246923E-013	4.8836529408321331E-013	4.9420840524846185E-013
4.8747310741388454E-013	4.9305435406340439E-013	4.8984378287075310E-013
4.9630428171283700E-013	4.8213488415743078E-013	4.7763838249688960E-013
4.3270360720013091E-013	5.3786977555049605E-013	4.5415199478922443E-013
5.3704635004198409E-013	4.5878353591278663E-013	5.3559776413255472E-013
...	...	...
...	...	...
...	...	...
4.8039684703802249E-013	5.2860623605878718E-013	5.1383718465251682E-013
5.4350730667712987E-013	5.1833737141194172E-013	5.7294181564914557E-013
5.2510989550484147E-013	4.5405735540370621E-013	7.2719187918391087E-013
5.4835967713254201E-013	7.4677153651523405E-013	5.6983384369558097E-013
7.3705268684215626E-013	6.0599347737544604E-013	7.2417501860889694E-013
6.2982611491556472E-013	7.1425990705449986E-013	6.3581089660082558E-013
6.9851982260008594E-013	6.3720118936763108E-013	6.8207052753756166E-013

B.7 Running Instructions

For performing the dynamics calculation in the KH frame for a potential system, the first task is to make the potential in the diagonal form, calculate its Fourier components and input it in the recursive subroutine. Following the compilation of the code using the compilation instructions in section B.3, the following command is used to run the code: *./a.out* > & *abc.out* &

References

[1] J. Backus, *"The history of Fortran 1, 2 and 3"*. Softwarepreservation.org. Retrieved 19 November 2014.

[2] E. Anderson, Z. Bai, C. Bischof, S. Blackford, J. Demmel, J. Dongarra, J. Du Croz, A. Greenbaum, S. Hammarling, A. McKenney, and D. Sorensen, *LAPACK Users' Guide*, Third edition, Society for Industrial and Applied Mathematics, 1999.

Appendix C

Atomic units

Length $a_0 = \frac{\hbar^2}{m_e e^2} = 5.29 \times 10^{-11}$ m (α_0 has a unit of length)

Charge $e = 1.602 \times 10^{-19}$ C

Energy $E_h = 27.21$ eV $= 1$ Hartree

Frequency $\nu_0 = \frac{v_0}{a_0} = 4.13 \times 10^{16}$ s^{-1} (v_0 = atomic unit of velocity)

Angular frequency $\omega = 2\pi\nu_0 = 1.51976 \times 10^{-16}$ rad/s

Electric field $E_0 = \frac{e}{4\pi\epsilon_0 a_0^2} = 5.14 \times 10^9$ V/cm

Electric field intensity $= \frac{\epsilon_0 c E_0^2}{2} = 3.51 \times 10^{16}$ W/cm^2 for peak E_0 field